Field Crops Research 242 (2019) 107581

Contents lists available at ScienceDirect

Field Crops Research

journal homepage: www.elsevier.com/locate/fcr

# A model-based approach to analyse genetic variation in potato using standard cultivars and a segregating population. I. Canopy cover dynamics

Muhammad Sohail Khan[a,b], Paul C. Struik[a,*], Peter E.L. van der Putten[a], Hans J. Jansen[c], Herman J. van Eck[d,e], Fred A. van Eeuwijk[c], Xinyou Yin[a]

[a] Centre for Crop Systems Analysis, Plant Sciences Group, Wageningen University, P.O. Box 430, 6700 AK Wageningen, the Netherlands
[b] Department of Horticulture, Faculty of Agriculture, Gomal University, Dera Ismail Khan, Khyber Pakhtunkhwa, Pakistan
[c] Biometris, Wageningen University, P.O. Box 100, 6700 AC Wageningen, the Netherlands
[d] Laboratory of Plant Breeding, Wageningen University, P.O. Box 386, 6700 AJ Wageningen, the Netherlands
[e] Centre for Biosystems Genomics, P.O. Box 98, 6700 AB Wageningen, the Netherlands

ARTICLE INFO

*Keywords:*
Haulm growth
Genotype-by-environment interaction
Heritability
Maturity type
QTL mapping

ABSTRACT

We designed a model to quantify the canopy cover dynamics in potato (*Solanum tuberosum* L.). It describes the dynamics during the build-up phase, maximum cover phase, and decline phase of canopy development through five parameters defining timing of three phases and maximum canopy cover ($v_{max}$). These five parameters were estimated for 100 individuals of an F1 population, their parents, and five standard cultivars, using data from six field experiments, and used to estimate secondary traits, related to duration and area under the canopy cover curve for the three phases. The duration of the canopy build-up phase ($D_{P1}$) was rather conserved, but the duration of maximum canopy cover ($D_{P2}$) and the decline phase ($D_{P3}$) varied greatly, with late maturing genotypes having longer $D_{P2}$ and $D_{P3}$ and thus a higher area under the canopy cover curve ($A_{sum}$). High genetic variability coupled with high heritability was recorded for end of canopy senescence ($t_e$), $D_{P2}$ and $A_{sum}$. Strong positive phenotypic and genetic correlations were observed between $D_{P2}$ and $t_e$, $v_{max}$ or $A_{sum}$ indicating that genotypes with longer $D_{P2}$ could be indirectly obtained by selecting for these traits. Several quantitative trait loci (QTLs) were detected for model traits explaining the variance by up to 74%. Clustering of many QTLs were found on position 18.2 cM on paternal linkage group V with major additive effects. Many additional QTLs with minor effects were mostly associated with maternal linkage groups. Our model approach could be used to exploit available genetic variability in canopy cover dynamics of potato.

## 1. Introduction

Tuber dry matter yield in potato (*Solanum tuberosum* L.) can be quantified by the summation of the daily incoming photosynthetically active radiation (PAR) times the daily fraction of that radiation intercepted by the crop times the radiation use efficiency times the daily fraction of the total dry matter partitioned to the tubers (Struik et al., 1990). This paper is on the first part of the equation: the fraction of the incoming radiation intercepted, as in many potato growing regions the ability of the crop to produce and maintain a green canopy able to absorb and use incoming radiation during the available growing season for biomass production determines tuber yields (Moll and Klemke, 1990; Haverkort and Struik, 2015).

The crop canopy cover at each time during the growing season is the resultant of the rate and duration of canopy growth and the rate of canopy senescence (or the timing of the haulm killing) (Struik et al., 1990; Struik, 2007). Under optimal conditions and with long growing seasons, early establishment of full canopy cover and its persistence over a long period lead to a higher yield due to better interception of incoming radiation (Martin, 1995), although the biomass needs to be partitioned to tubers in order to obtain economic yield. There is a close and positive correlation between canopy cover and tuber yield (Van der Zaag, 1982; Vander Zaag and Demagante, 1987; Fahem and Haverkort, 1988; Haverkort and Struik, 2015). The proper quantification of canopy dynamics is therefore one of the most important elements of modelling potato production (Hodges, 1991).

Genotypic differences in potato canopy cover are large (Spitters, 1988; Jefferies and MacKerron, 1993; Tourneux et al., 2003; Ospina et al., 2014). Like many other complex quantitative traits, canopy cover may be controlled by many interacting genes of which each only has a

* Corresponding author.
*E-mail address:* paul.struik@wur.nl (P.C. Struik).

https://doi.org/10.1016/j.fcr.2019.107581
Received 31 December 2018; Received in revised form 18 July 2019; Accepted 23 July 2019

small effect (Lark et al., 1995; Orf et al., 1999; Daniell and Dhingra, 2002; Stuber et al., 2003). Canopy cover dynamics also show a high genotype-by-environment (G × E) interaction (Pashiardis, 1987; Allen and Scott, 1992; Schittenhelm et al., 2006).

The main environmental factors influencing the canopy dynamics under field conditions are temperature, photoperiod, light intensity, water supply, and nitrogen (N) supply. For our study the effects of temperature and N are most relevant and these are therefore summarised in this introduction. Temperature strongly influences stem elongation and branching (Marinus and Bodlaender, 1975; Allen and Scott, 1980; Struik et al., 1989; Almekinders and Struik, 1994, 1996) and leaf appearance, expansion, and senescence (Kirk and Marshall, 1992; Vos, 1995a; Firman et al., 1995; Struik and Ewing, 1995; Van Delden et al., 2001; Fleisher and Timlin, 2006; Fleischer et al., 2006; Struik, 2007), with optimal and maximum daytime air temperatures for these processes contributing to canopy development being about 23–25 °C and about 32 °C, respectively (Struik, 2007). N supply affects the number of lateral (basal and sympodial) branches, the number of leaves on those branches, the individual leaf size and leaf senescence (Fernando, 1958; Humphries and French, 1963; Vos and Biemond, 1992; Almekinders and Struik, 1996). Nitrogen helps to attain complete canopy cover early in the season, especially under relatively resource-poor conditions (Haverkort and Rutavisire, 1986; Vos, 2009), to extend the period of full canopy cover; and to slow down senescence (Santeliz and Ewing, 1981), thus leading to increased light interception (Martin, 1995).

There is a clear need to investigate the components of genetic variation (e.g. in canopy dynamics) and to determine the G × E interaction for a diverse population under contrasting environmental conditions (Tarn et al., 1992; Bradshaw, 1994). The genetic variation and the G × E interaction for canopy cover need to be defined by precisely quantifying the complex dynamics of canopy cover across diverse environments and dissecting it into component traits. Such component traits need to be optimised in such a way that the crop can complete its growth cycle within the period of favourable weather conditions thus realising a high yield and an adequate harvest index. There is a growing awareness that in order to better analyse complex traits using increasingly available genomic information, integration of quantitative crop physiology with genetics is required (Yin et al., 1999a, 1999b; Tardieu, 2003; Yin et al., 2004; Hammer et al., 2006; Yin and Struik, 2008; Chenu et al., 2009; Messina et al., 2009; Hammer et al., 2010; Tardieu and Tuberosa, 2010; Yin and Struik, 2010; Yin et al., 2018).

In this paper, we first describe a quantitative approach to analyse the time course of canopy cover during the entire crop cycle as a function of thermal time and its variability among potato genotypes and to break the time course and its variation down into biologically meaningful and genetically relevant component traits. Using this approach, we quantitatively analyse the sources of variation in canopy cover dynamics among full-sibs of an outcrossing segregating population, their parents and a set of standard cultivars of potato. The heritability of and genetic variation among different component traits of canopy cover are estimated (Van Eeuwijk et al., 2005). Finally, we perform QTL mapping of our traits to investigate their genetic basis and discuss the co-locations of QTLs for these traits and their QTL-by-environment (QTL × E) interaction. With such information, dominant components of canopy cover can be identified and their phenotypic and genetic correlations can be assessed, with the ultimate goal of designing an effective breeding strategy of potato.

## 2. Materials and methods

### 2.1. F1 segregating population of SH × RH and standard cultivars

The plant material used in this study consisted of 100 F1 diploid ($2n = 2x = 24$) potato genotypes derived from a cross between two diploid heterozygous potato clones, SH83-92-488 × RH89-039-16 (Rouppe van der Voort et al., 1997; Van Os et al., 2006) referred to as SH × RH. This population is well adapted to the growing conditions of the Netherlands and segregates for maturity (Van der Wal et al., 1978; Van Oijen, 1991). Besides, we also used five standard cultivars with very different maturity types (i.e. Première, Bintje, Seresta, Astarte, and Karnico) as check genotypes and to allow a benchmarking of consequences of maturity type on the time course of canopy cover.

### 2.2. Field experiments and measurements

Six field experiments were carried out in Wageningen, the Netherlands (52 °N latitude), during 2002, 2004, and 2005, with two experiments in each year, to record canopy cover dynamics for 100 F1 genotypes, 2 parents, and 4 (Exps 5 and 6) or 5 (Exps 1–4) standard cultivars. Karnico was not included in the two experiments during 2005. Experiments differed in environmental conditions because they were carried out in different years, on different soils and under different N fertiliser regimes, thereby creating six contrasting environments (Table 1). Each experiment was conducted using a randomised complete block design with two blocks. The genotypes were randomised

**Table 1**
Description of the experimental sites and experimental methods applied in Wageningen, the Netherlands.

| Experiment | 1 | 2 | 3 | 4 | 5 | 6 |
|---|---|---|---|---|---|---|
| Year | 2002 | 2002 | 2004 | 2004 | 2005 | 2005 |
| Soil type | Clay | Sand | Clay | Sand | Sand | Sand |
| Planting pattern (m × m) | 0.75 × 0.30 | 0.75 × 0.30 | 0.75 × 0.27 | 0.75 × 0.27 | 0.75 × 0.27 | 0.75 × 0.27 |
| Planting date | 25 April | 25 April | 28 April | 28 April | 4 May | 26 April |
| Plant density (plants $m^{-2}$) | 4.44 | 4.44 | 4.94 | 4.94 | 4.94 | 4.94 |
| Net plot size ($m^2$) | 22.95 | 22.95 | 20.66 | 20.66 | 20.66 | 20.66 |
| Soil N at planting (kg $ha^{-1}$) | n.d.[1] | n.d.[2] | 12.5 | 23.0 | 81.0 | 49.5 |
| Fertiliser N (kg $ha^{-1}$) | 143 | 175 | 70 | 200 | 125 | 50 |
| Tuber N uptake (kg $ha^{-1}$) [3] | – | – | 112.3 | 172.0 | 153.6 | 156.1 |
| Weather conditions during growing season | | | | | | |
| | | 2002 | | 2004 | | 2005 |
| Air temperature max. (°C) | | 20.9 | | 20.6 | | 20.7 |
| Air temperature min. (°C) | | 11.2 | | 10.4 | | 9.9 |
| Rainfall (mm) | | 364 | | 367 | | 369 |
| Relative humidity (%) | | 78.2 | | 75.6 | | 76.5 |
| Solar radiation (MJ $m^{-2}$ $d^{-1}$) | | 15.3 | | 15.8 | | 15.8 |

[1] n.d. = no data. Guestimate: 40 kg N $ha^{-1}$.
[2] n.d. = no data. Guestimate: 60 kg N $ha^{-1}$.
[3] Data for Experiments 1 and 2 were not available and replaced by "–".

within each block, consisting of 106 or 107 plots. Each plot had six rows of 16–18 plants. The seed bed was prepared following standard cultivation practices. Seed tubers were planted in rows spaced 0.75 m apart with 0.27–0.30 m between plants within the same rows. N fertiliser was broadcasted at planting in amounts depending on experiment (Table 1). Soil phosphorus and potassium levels were kept sufficiently high to sustain normal crop growth. Crops were managed well to ensure that they were free of pests, diseases, and weeds. Irrigation was applied when necessary to avoid drought stress.

Plant emergence date was observed as the date when 50% of the plants had emerged from the soil surface. Afterwards, green canopy cover (%) was visually assessed on a weekly basis for each plot during the whole crop cycle by using a grid as described by Burstall and Harris (1983). The grid consisted of an aluminium frame with the dimensions 0.75 m × 0.90 m, adjusted to the common planting pattern for potato (row width 0.75 m, planting distance within the row 0.30 m). The frame was divided into 100 equal rectangles of 0.075 m × 0.090 m. The grid was placed above the potato canopy at 1 m from the ground and only those rectangles more than half filled with green leaves were counted by observing vertically above to avoid parallax error (Cadersa and Govinde, 1999). The grid was placed half way on each side of the potato row to sample three plant positions. Observations were always made at the same position in the field. The number of observations made on the canopy cover during the growing season per individual plot was 17–21.

At the end of the growing season, tubers of each plot were harvested and dried in an oven at 70 °C to constant weight. In samples of the growing seasons of 2004 and 2005, tuber nitrogen content was determined by micro-Kjeldahl digestion and distillation (Association of Official Analytical Chemistry (AOAC, 1984) in a fully accredited commercial laboratory. Average N uptake was calculated and was used to characterise some of the environments in terms of total N available for crop growth.

### 2.3. Model approach

#### 2.3.1. A model for phasic development of canopy cover dynamics

Canopy cover dynamics in potato as quantified by the grid method typically follows a pattern that can be subdivided into three distinct phases (Fig. 1), i.e. a build-up phase (*P*1), a maximum cover phase (*P*2), and a decline phase (*P*3).

#### 2.3.2. Build-up phase (P1)

This first phase covers the period from emergence to maximum canopy cover, and is dominated by appearance of stems, lateral branches and leaves, and expansion of those organs (Allen and Scott, 1992; Vos and Biemond, 1992; Vos, 1995a; Fleisher et al., 2006). To obtain flexible and asymmetrical curves, canopy cover during *P*1 can be written, according to a sigmoid part of the function for determinate growth (Yin et al., 2003), as:

$$v = v_{\max}\left(1 + \frac{t_1 - t}{t_1 - t_{m1}}\right)\left(\frac{t}{t_1}\right)^{\frac{t_1}{t_1 - t_{m1}}} \quad \text{with} \quad 0 \le t \le t_1 \tag{1}$$

where $t_{m1}$ is the inflexion point and $v_{\max}$ is the maximum value of canopy cover $v$, which is reached at time $t_1$ (Fig. 1). Eq. (1) can be applied to canopy cover within the time span of $0 \le t \le t_1$; otherwise, $v$ has to be set at 0 if $t < 0$ or at $v_{\max}$ if $t > t_1$.

#### 2.3.3. Maximum cover phase (P2)

During this phase the canopy cover retains its maximum level $v_{\max}$. The canopy cover during *P*2 is simply given by:

$$v = v_{\max} \quad \text{with} \quad t_1 < t < t_2 \tag{2}$$

where $t_2$ reflects the last time point when canopy cover is still at its maximum and/or onset of canopy senescence (Fig. 1).

#### 2.3.4. Decline phase (P3)

The canopy cover starts to decline after time $t_2$, and reaches zero at the end of the crop cycle, i.e. $t_e$. Usually this decline follows a reversed sigmoid pattern, which could be formulated as $v_{\max}\,[1 - f(t)]$ (cf. Yin et al., 2009), where $f(t)$ is the function, such as Eq. (1), describing a normal sigmoid pattern with time. Therefore, for *P*3, an equation could be formulated, using an inflexion point of the decline phase. However, in many cases the estimates for parameters showed large standard errors, indicating over-fitting when a model having this inflexion is applied in combination with Eqs. (1) and (2) to describe the data of the entire time course of canopy dynamics. To reduce the chance of over-

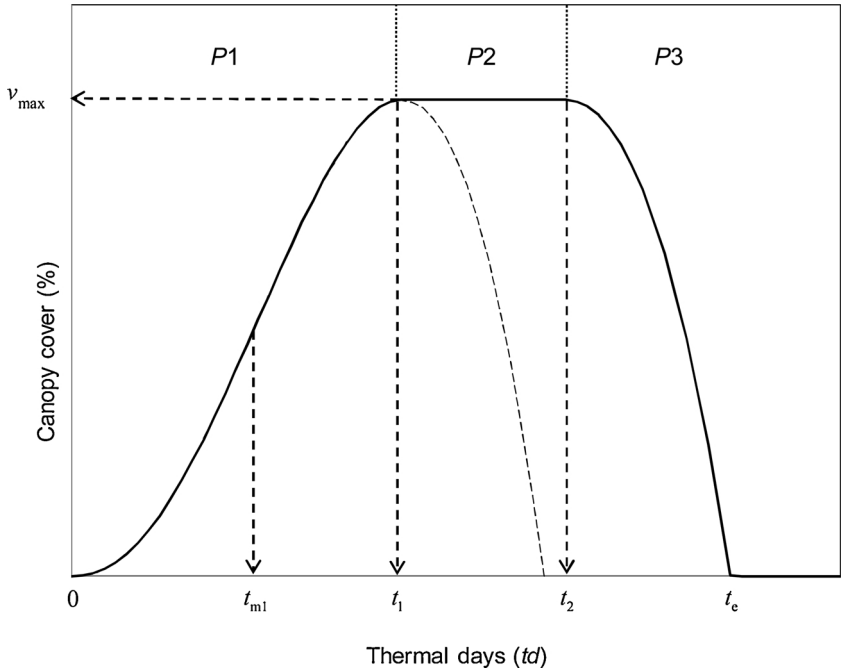


**Fig. 1.** Temporal course of potato canopy development (full curve) from time 0 to $t_e$ described by our three-phase model, Eqs. (1–3), respectively. *P*1 (canopy build-up phase), *P*2 (maximum canopy cover phase), and *P*3 (canopy decline phase). The dashed curve is the mathematical extension of Eq. (1).

fitting, we developed an equation for the canopy cover in the decline phase (i.e. *P*3) thereby excluding this second inflexion, yet yielding satisfactory results:

$$v = v_{max}\left(\frac{t_e - t}{t_e - t_2}\right)\left(\frac{t + t_1 - t_2}{t_1}\right)^{\frac{t_1}{t_e - t_2}} \quad \text{with } t_2 \le t \le t_e \tag{3}$$

where $t_e$ reflects the last time point when canopy cover is zero. This equation is based on a decline part of the equation of Yin et al. (1995) and Yin et al. (2005) but with a restriction that $t_e$ differs from the extended end point of Eq. (1) by $(t_2 - t_1)$ (Fig. 1). Eq. (3) can be applied within the time span of $t_2 \le t \le t_e$; otherwise, $v$ has to be set at 0 if $t > t_e$.

Combining Eqs. (1, 2, and 3) yields a model with five parameters: $t_{m1}$, $t_1$, $t_2$, $t_e$, and $v_{max}$. Any further reduction of parameters resulted in significant loss of fit (data not shown). The model describes canopy dynamics for a given genotype-environment combination. The model contains three segments, but is smooth, because the first derivatives of $v$ with respect to $t$ are zero at the joining points $t_1$ and $t_2$. Values of model parameters $t_{m1}$, $t_1$, $t_2$, $t_e$, and $v_{max}$ were estimated for each genotype of every experiment with the iterative non-linear least-square regression using the Gauss method, as implemented in the PROC NLIN of the SAS software (SAS Institute Inc., 2004).

Once model parameters were estimated, several secondary traits can be derived (Khan, 2012; Khan et al., 2013) reflecting the duration of the canopy cover phases *P*1, *P*2, *P*3 (i.e. $D_{P1}$, $D_{P2}$, $D_{P3}$, respectively), the rates of canopy cover dynamics (i.e. $c_{m1}$, maximum growth rate during *P*1; $c_1$, average growth rate for *P*1, $c_3$, average senescence rate during $P_3$), area under the green canopy curve for above mentioned three phases (i.e. $A_1$, $A_2$, $A_3$, respectively) and area under the whole green canopy curve (i.e. $A_{sum}$). The latter reflects the overall potential of a crop to intercept solar radiation during the whole growing season (cf. Vos, 1995b, 2009) and could be used as indicator of crop maturity (Khan et al., 2013). The time variables and duration were expressed in terms of thermal days (*td*) to account for the influence of daily and seasonal air temperature fluctuations under field conditions (McMaster and Wilhelm, 1997; Yin et al., 2005). These data sets created the basis for the estimation of physiological traits describing the dynamics of canopy development for a large set of F1 segregating population and standard cultivars. For details about the calculation of secondary traits and thermal day approach, see Supplementary material, Ellis et al. (1990), and Khan (2012). In this paper, we will not use all secondary traits to keep the paper within reasonable limits.

### 2.4. Statistical and genetic analyses

All statistical analyses were performed in Genstat (Payne et al., 2009). A general analysis of variance across environments was performed to test the significance and extent of differences among environments, all genotypes (including the F1 population, the parents, and standard cultivars) and G × E interactions, where the effect of block within environment was included in the model. Means of genotype (G), environment (E) and G × E interaction terms were compared using the Fisher's least significant difference (LSD) test. Further statistical analyses were performed using only the 100 genotypes of the F1 population and these are described below.

#### 2.4.1. Estimation of variance components

We used a statistical model (Van Eeuwijk, 2003) to estimate the variance components and to assess the contribution of genotypic main effects and the G × E to the total phenotypic variance for our model traits:

$$\underline{y}_{ijk} = \mu + \underline{E}_j + \underline{\beta}_{jk} + \underline{G}_i + \underline{GE}_{ij} + \underline{\varepsilon}_{ijk} \tag{4}$$

where $i = 1,\ldots,100$; $j = 1,\ldots,6$; $k = 1, 2$; and $\underline{y}_{ijk}$ denotes the response variable of genotype $i$, in environment $j$, block $k$; $\mu$ is the grand mean; $\underline{E}_j$ is the environmental main effect; $\underline{\beta}_{jk}$ stands for block within environment effect; $\underline{G}_i$ is the genetic effect of genotype $i$; $\underline{GE}_{ij}$ is the genotype-by-environment interaction effect for genotype $i$ in environment $j$, and $\underline{\varepsilon}_{ijk}$ is a residual term. The underlined terms were considered as random effects, which were assumed to be normally and independently distributed with zero mean and a proper variance.

The restricted maximum likelihood (REML) procedure was used to estimate the variance components. The significance of the variance components was tested using the likelihood ratio (LR) test (Morrell, 1998). The phenotypic variance ($\sigma^2_{Ph}$) was estimated from these variance component estimates as (Bradshaw, 1994; Falconer and Mackay, 1996; Lynch and Walsh, 1998):

$$\sigma^2_{Ph} = \sigma^2_E + \sigma^2_\beta + \sigma^2_G + \sigma^2_{GE} + \sigma^2_\varepsilon \tag{5}$$

where $\sigma^2_E$ = environmental variance, $\sigma^2_B$ = block variance, $\sigma^2_G$ = genetic variance, $\sigma^2_{GE}$ = G × E variance, and $\sigma^2_\varepsilon$ = experimental error variance.

#### 2.4.2. Phenotypic and genetic coefficient of variation

Scaling of the variance by the trait mean, i.e. calculating the coefficient of variation provides a more appropriate way to compare traits (Johnson et al., 1955; Houle, 1992). We therefore calculated the coefficient of variation (%) for each model parameter and derived trait across six experiments, according to:

$$CV_X = \frac{\sqrt{\sigma^2_X}}{\mu} \times 100 \tag{6}$$

where $\mu$ is the grand mean of the population, and $\sigma^2_X$ is a variance component (i.e. $\sigma^2_{ph}$ or $\sigma^2_G$ or $\sigma^2_E$ or $\sigma^2_{GE}$) from Eq. (4).

#### 2.4.3. Phenotypic and genetic correlation

Product-moment (Pearson) correlations among model traits were calculated using genotypic means across all six environments. The genetic correlations were estimated using the following equation (Holland, 2006):

$$r_{Gij} = \frac{\sigma^2_{Gij}}{\sqrt{\sigma^2_{Gi}\sigma^2_{Gj}}} \tag{7}$$

where $\sigma^2_{Gij}$ is the estimated genetic covariance between traits $i$ and $j$; $\sigma^2_{Gi}$ and $\sigma^2_{Gj}$ are the genetic variances of traits $i$ and $j$, respectively. The multivariate REML procedure was used to estimate the genetic variance and covariance estimates (Meyer, 1985; Holland, 2006). The significance of genetic correlations was determined using a *t*-test after a *z*-transformation of the correlation coefficients (Sokal and Rohlf, 1995; Gutteling et al., 2007).

#### 2.4.4. Heritability

We estimated the broad-sense heritability ($H^2$) (%) across all six environments by using the estimated variance components of the linear model described as per Eq. (4), through the following equation (Bradshaw, 1994; Falconer and Mackay, 1996):

$$H^2 = \frac{\sigma^2_G}{\sigma^2_G + \frac{\sigma^2_{GE}}{n_e} + \frac{\sigma^2_\varepsilon}{n_t}} \times 100 \tag{8}$$

where $n_e = 6$ represents the number of environments, and $n_t = 12$ is the product of number of blocks and environments.

The broad-sense heritability ($H^2$) was also estimated for each individual experiment by using the following formula (Bradshaw, 1994):

$$H^2 = \frac{\sigma^2_G}{\sigma^2_G + \frac{\sigma^2_\varepsilon}{n_b}} \times 100 \tag{9}$$

where $\sigma^2_G$ = genetic variance; $\sigma^2_\varepsilon$ = experimental error variance, and $n_b = 2$ represents the number of blocks per individual environment.

The variance components were estimated per individual trial basis.

#### 2.4.5. Extension of an AFLP marker map of the SH × RH population

The AFLP primer combinations used in this study have been previously applied to create the ultra-dense genetic map of 130 SH × RH genotypes as described in Van Os et al. (2006). As our 100 F1 lines were only partly genotyped for creating that map, 120 new SH × RH genotypes were fingerprinted with AFLP™ (Vos et al., 1995) to make a map for 250 individuals. Genomic DNA was extracted from frozen leaf tissue according to Van der Beek et al. (1992). AFLP markers were generated according to standard protocols with radioactive labels, using four $E_{co}$-$M_{se}$ primer combinations (Vos et al., 1995). The AFLP profiles of the parental clones were compared with an ultra-dense genetic map and AFLP products of equal electrophoretic mobility which segregated in both sets of the lines were identified. The AFLP (only 1:1 segregating markers) were first mapped in the SH × RH mapping population using JoinMap 4.1 (Van Ooijen, 2006) using a bin mapping approach (Van Os et al., 2006). The marker data were split into two sets on the basis of their segregation type. Markers that were heterozygous in the maternal parent (SH) and absent in the paternal parent (RH) were scored as < ab × aa > ; "paternal" markers heterozygous in RH and absent in SH were scored as < aa × ab > .

For map construction, recombination frequencies were converted into map units (cM) by the use of the Kosambi function. Only markers with a recombination value of ≤ 0.25 were considered as described by Van Os et al. (2006). The maternal and paternal data sets were divided into 12 and 13 linkage groups, respectively. A graphic representation of a map was made by the Map Chart software (Voorrips, 2002). The relative positions of markers and QTLs on the linkage maps can be used to identify the approximate physical position of these QTL on the potato reference genome (Xu et al., 2011), because this mapping population is identical to the genetic map used to anchor the sequences of the reference genome into pseudomolecules. Data to convert genetic positions into physical positions were described by Sharma et al. (2013).

#### 2.4.6. QTL detection

Genstat version 14 (Payne et al., 2009) software was used to identify possible QTL(s) for our model traits. Eighty-eight genotypes of our 100 F1 lines were covered in the sample of the aforementioned 250 lines of SH × RH population for the extended marker map; data of these 88 lines were therefore used for detection of QTLs for five model parameters and nine secondary traits. QTL analysis was performed individually for all six experiments (environments).

QTL models were fitted for the two parents separately. Initially, the conventional Simple Interval Mapping (SIM) procedure as described by Lander and Botstein (1989) and Hackett et al. (2001) was used to scan the genome for the major QTLs per individual environment. A QTL was declared to be significant ($P < 0.05$) for the threshold value ($-\log_{10}(P) > 3.4$). Secondly, a more sophisticated QTL mapping procedure, the Composite Interval Mapping (CIM) was performed to increase the reliability of the QTL analysis (Jansen, 1993; Jansen and Stam, 1994; Zeng, 1994; Jansen, 1995). In this method, background markers were selected to take over the role of the putative QTLs as cofactors to reduce the residual variance. In our analysis, background markers closest to the indicated region of putative QTLs with $-\log_{10}(P)$ scores exceeding the threshold were gradually used as cofactors. This procedure was repeated until no further QTLs were found. The percentage of the total phenotypic variation explained by QTLs identified for each trait was estimated as the $R^2$-value.

## 3. Results

### 3.1. Model performance in describing canopy cover dynamics of potato

The use of data in thermal days resulted in a more stable parameter estimation than the use of data in days (data not shown), as the confounding effects of diurnal and seasonal air temperature fluctuations during the experimental periods could effectively be removed using thermal days. The model for the canopy cover dynamics (i.e. combined Eqs. (1, 2, and 3)) fitted well for each genotype of the potato segregating population, their parents and standard cultivars in the entire data set, with $R^2$ values ranging from 0.94 to 1.00 (n = 17–21; data not shown). Fig. 2 shows the curve-fitting results for the SH and RH parents and for the standard cultivars that were present in each experiment. In most cases, the standard error (SE) values for observed points (i.e. average of two blocks) were much higher during the canopy decline phase than during the first two phases; the estimation of $t_e$ also involved much extrapolation due to fewer data points in the third phase of canopy growth.

### 3.2. Assessment of model parameters and secondary traits

Usually, the estimated values of each model parameter and secondary trait differed very little between the two blocks and there was a good positive linear correlation between the two blocks for all model parameters ($R^2$ values usually above 0.70; n = 107). Table 2 presents mean values of these traits for the two parents (SH and RH), and five standard cultivars across six environments. Due to page limitation, we only discuss here data for a few selected model traits viz. $t_e$, $\nu_{max}$, $D_{P1}$, $D_{P2}$, $D_{P3}$ and $A_{sum}$. The other traits are closely related to the selected ones.

Potato cultivars varied significantly ($P < 0.05$) in the duration of the entire crop cycle which is reflected in variation in $t_e$ (Table 2). Late cultivars gave higher values for $t_e$ followed by mid-late and early cultivars. There were small differences among the cultivars for $\nu_{max}$, but under certain environmental conditions late cultivars showed higher values than earlier ones, because haulm growth continued longer. The initial phase of canopy growth (i.e. $D_{P1}$) was not much affected by the maturity type of genotypes, but there were very large differences among standard cultivars for the duration of *P*2 and *P*3 (i.e. $D_{P2}$ and $D_{P3}$, respectively). The duration of *P*2 ($D_{P2}$) tended to be longer for late maturing cultivars. Mean estimates for $A_{sum}$ ranged from 3051 to 6207 % *td* for the five standard cultivars and two parental genotypes (Table 2). $A_{sum}$ values were higher for late cultivars like Karnico and Astarte than for early cultivars such as Première (Table 2). A larger area during *P*2, i.e. $A_2$, significantly contributed to the higher values of $A_{sum}$ in late cultivars (data not shown).

Mean values of model traits also showed highly significant ($P < 0.01$) variation within the F1 population across the six environments (Table 2). The variation (the median, minimum, and maximum values) of these model traits for the F1 population per individual experiment is illustrated by Fig. 3. Wide ranges of variation were observed for duration of the three phases of canopy cover i.e. $D_{P1}$ in Exp. 3, for $D_{P2}$ in Exp. 4, and for $D_{P3}$ in Exp. 2. In the case of $A_{sum}$, the ranges were highest in Exp. 3 and values were between 1030 and 6101 % *td* (Fig. 3). These results were in line with the results for the length of the three canopy cover phases $D_{P1}$, $D_{P2}$, and $D_{P3}$. Within the F1 population, SHRH34-H6, SHRH83-L9, and SHRH-136 recorded the highest average $A_{sum}$ with values of 6146, 5836, and 5739 % *td*, respectively. These genotypes especially out-performed the other ones in the low N environment (i.e. Exp. 3).

### 3.3. Phenotypic, genetic and environmental variances

Table 3 presents estimated values of phenotypic, genetic, and environmental variances for our model traits in the F1 population. Almost all components of variance were significant ($P < 0.01$) (Table 3). The major portion of the phenotypic variance was accounted for by the genetic variance component for $t_e$ and $A_{sum}$ indicating the genetic basis of variation within F1 population for these traits (Table 3). The contribution of the environmental variance to the phenotypic variance was relatively large for $\nu_{max}$, $D_{P1}$, and $D_{P2}$. The contribution of the G × E

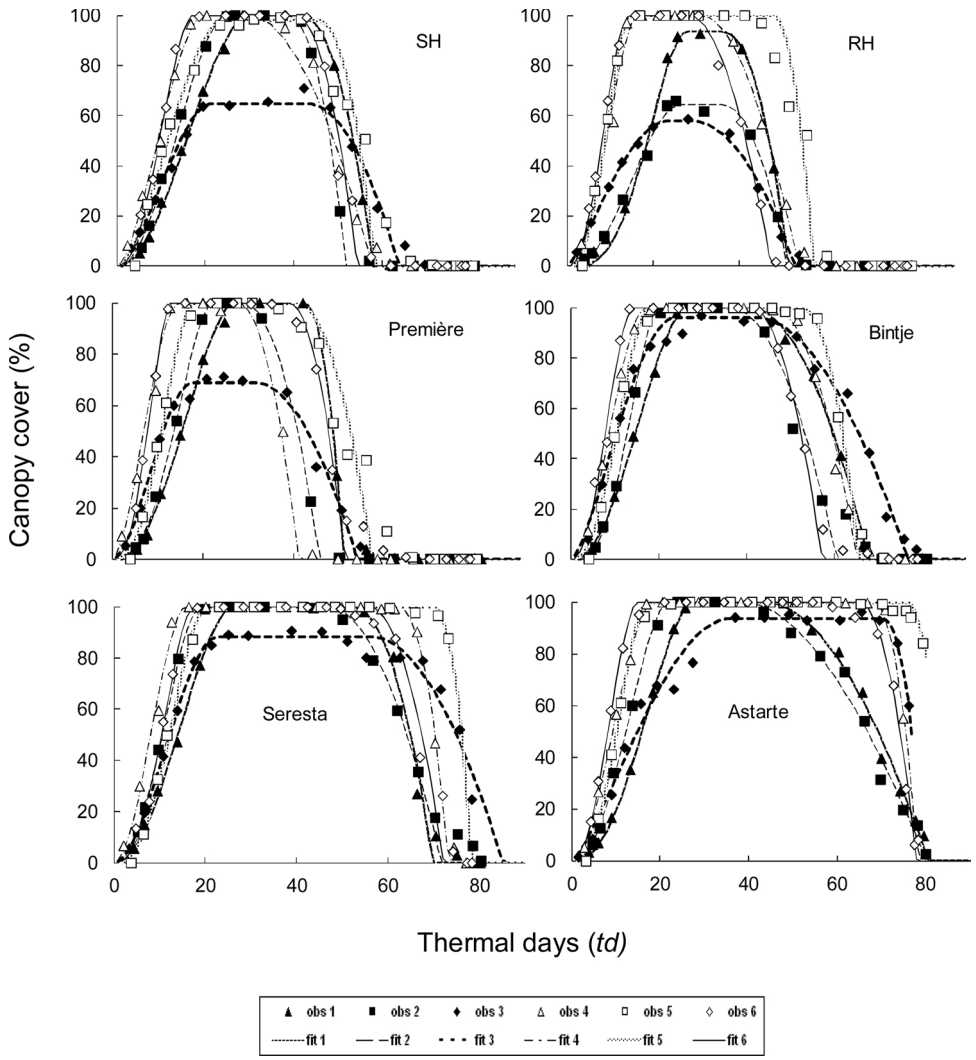


**Fig. 2.** Observed (obs) points and fitted (fit) curves of SH and RH parents and four standard cultivars for all six experiments (environments).

interaction variance component to the phenotypic variance was large for $D_{P3}$ (Table 3).

Estimates of phenotypic ($CV_{Ph}$), genetic ($CV_G$), environmental ($CV_E$), and G × E interaction ($CV_{GE}$) coefficients of variation across the six experiments are presented in Table 4. Estimates of $CV_{Ph}$ ranged from 15.4% to 65.1%. These estimates were smallest for $t_e$ and $v_{max}$ and highest for $D_{P2}$. Traits with higher $CV_{Ph}$ exhibit more total variance and are useful as selection criteria in breeding provided the trait is also heritable. Our F1 population reflected high $CV_G$ for almost all traits except for $v_{max}$ and $D_{P1}$. Relatively high $CV_G$ and low $CV_E$ estimates were obtained for $t_e$ and $A_{sum}$ suggesting that these traits, compared with the other ones, are under a greater influence of genetic control. The $CV_E$ was comparatively higher than $CV_G$ for traits $v_{max}$, $D_{P1}$, $D_{P2}$, and $D_{P3}$, thus reflecting environmental sensitivity of these traits. The $CV_{GE}$ ranged from 4.3% to 25.6% among the traits. The $CV_{GE}$ exceeded the $CV_G$ for traits $v_{max}$, $D_{P1}$ and $D_{P3}$. These results show the major contribution of G × E to the $CV_{Ph}$ of these traits in our experiments.

### 3.4. Phenotypic and genetic correlations of model traits

The results showed variation in the relationship among model traits across individual experiments. In most experiments, there were strong negative phenotypic correlations between $D_{P1}$ and $D_{P2}$. The correlations between $D_{P2}$ and $D_{P3}$ were mostly weak and non-significant, only Exps 3 and 4 showed significant ($P < 0.05$) and strong ($r = -0.59$) negative correlations (Table 5). These results suggest that genotypes with slow canopy build-up had a relatively short period of maximum canopy cover ($D_{P2}$). Furthermore, $D_{P1}$ and $D_{P2}$ also depended upon $v_{max}$, with $D_{P1}$ generally being long with a low $v_{max}$ but with $D_{P2}$ generally being short when $v_{max}$ was below 100%, whereas $D_{P2}$ could be (much) longer when the canopy reached 100% cover. The results further revealed strong positive correlations between $D_{P2}$ and $t_e$, whereas in half of the experiments $D_{P3}$ and $t_e$ were positively correlated. This suggests that both $D_{P2}$ and $D_{P3}$ contribute positively to higher values of $t_e$. Later cultivars tended to senesce more slowly (i.e. tended to have a longer $D_{P3}$) than earlier cultivars. The results further indicated that traits $t_e$, $v_{max}$, and $D_{P2}$ positively contributed to the high values of $A_{sum}$ due to their strong, positive correlation with $A_{sum}$ in nearly all the experiments. These underline the important contribution of variation in these traits to variation in $A_{sum}$.

Table 5 also illustrates the genetic correlation coefficients between the model parameters and secondary traits within the F1 population. The results revealed weak genetic correlations between $D_{P1}$ and $D_{P2}$ in Exps 2, 3, and 6, whereas Exps 1, 4, and 5 showed strong negative correlations (Table 5). The genetic correlations between $D_{P2}$ and $D_{P3}$ were mostly weak and non-significant, only Exp. 5 showed a significant negative genetic correlation with $r = -0.79$. There were strong positive genetic correlations between $D_{P2}$ and $v_{max}$ in all the experiments except in Exps 3 and 6. The trait $D_{P2}$ also showed strong positive genetic correlations with $t_e$ in all experiments. About half of the experiments

**Table 2**
Estimated mean values of model traits as obtained from across environment ANOVA for the two parents (SH and RH), five standard cultivars (listed in order of increasingly longer crop cycle) and the mean of the F1 population. *td* stands for thermal day. Data for cv. Karnico were not available in Exps 5 and 6 and are replaced by "–".

| Parameter | Exp. 1 | Exp. 2 | Exp. 3 | Exp. 4 | Exp. 5 | Exp. 6 | Mean [1] |
|---|---|---|---|---|---|---|---|
| $t_e$ (*td*) | | | | | | | |
| SH | 57.8 | 51.8 | 63.7 | 57.8 | 58.2 | 54.4 | 57.3 e |
| RH | 51.3 | 51.1 | 52.9 | 53.8 | 57.1 | 47.4 | 52.3 f |
| Première | 50.8 | 45.7 | 54.0 | 41.3 | 57.3 | 51.3 | 50.1 f |
| Bintje | 67.7 | 60.6 | 76.9 | 65.3 | 65.5 | 57.2 | 65.5 d |
| Seresta | 69.7 | 71.7 | 85.2 | 73.3 | 78.3 | 72.1 | 75.0 c |
| Astarte | 80.6 | 80.2 | 79.4 | 78.3 | 84.5 | 78.0 | 80.2 b |
| Karnico | 82.9 | 82.5 | 87.5 | 90.4 | – | – | 85.8 a |
| Mean [2] | 65.8 c | 63.4 d | 71.4 a | 65.7 c | 66.8 b | 60.1 e | |
| F1 mean [3] | 58.2 c | 53.4 e | 62.1 b | 58.1 c | 64.9 a | 57.2 d | |
| $v_{max}$ (%) | | | | | | | |
| SH | 100.0 | 100.0 | 64.7 | 100.0 | 98.0 | 100.0 | 93.8 c |
| RH | 93.6 | 64.2 | 57.8 | 100.0 | 100.0 | 100.0 | 85.9 d |
| Première | 100.0 | 100.0 | 68.9 | 99.8 | 100.0 | 100.0 | 94.8 bc |
| Bintje | 100.0 | 100.0 | 96.1 | 100.0 | 100.0 | 100.0 | 99.4 ab |
| Seresta | 100.0 | 99.9 | 88.2 | 100.0 | 100.0 | 100.0 | 98.0 abc |
| Astarte | 100.0 | 100.0 | 93.6 | 100.0 | 100.0 | 100.0 | 98.9 ab |
| Karnico | 100.0 | 100.0 | 100.0 | 100.0 | – | – | 100.0 a |
| Mean [2] | 99.1 b | 94.9 c | 81.3 d | 100.0 a | 99.7 ab | 100.0 a | |
| F1 mean [3] | 95.3 d | 99.2 ab | 71.0 e | 98.8 b | 97.5 c | 99.9 a | |
| $D_{P1}$ (*td*) | | | | | | | |
| SH | 30.1 | 25.0 | 21.5 | 19.9 | 24.1 | 17.4 | 23.0 a |
| RH | 27.6 | 26.1 | 23.6 | 16.5 | 14.7 | 14.4 | 20.5 ab |
| Première | 27.2 | 22.3 | 17.6 | 14.9 | 18.0 | 13.3 | 18.9 b |
| Bintje | 26.8 | 20.2 | 23.8 | 17.2 | 17.8 | 14.4 | 20.0 ab |
| Seresta | 26.3 | 19.1 | 22.6 | 15.9 | 20.1 | 17.7 | 20.3 ab |
| Astarte | 27.9 | 22.1 | 36.0 | 18.6 | 17.0 | 15.1 | 22.8 a |
| Karnico | 23.6 | 19.2 | 31.2 | 16.9 | – | – | 22.7 a |
| Mean [2] | 27.1 a | 22.0 c | 25.2 b | 17.1 e | 18.6 d | 15.4 f | |
| F1 mean [3] | 31.0 a | 23.0 d | 25.8 b | 19.7 e | 23.8 c | 16.4 f | |
| $D_{P2}$ (*td*) | | | | | | | |
| SH | 11.3 | 13.6 | 21.5 | 9.8 | 21.3 | 22.9 | 16.7 c |
| RH | 8.5 | 9.8 | 5.3 | 14.5 | 33.0 | 13.8 | 14.2 c |
| Première | 15.0 | 6.2 | 14.1 | 13.3 | 22.7 | 25.6 | 16.1 c |
| Bintje | 13.7 | 16.3 | 18.4 | 28.7 | 34.7 | 26.7 | 23.1 b |
| Seresta | 25.8 | 27.9 | 33.6 | 46.5 | 49.7 | 38.1 | 36.9 a |
| Astarte | 15.4 | 16.7 | 34.3 | 49.4 | 58.8 | 49.8 | 37.4 a |
| Karnico | 8.1 | 9.3 | 43.8 | 55.4 | – | – | 29.1 b |
| Mean [2] | 14.0 e | 14.2 e | 24.4 d | 31.1 b | 36.7 a | 29.5 c | |
| F1 mean [3] | 10.7 d | 11.1 cd | 12.0 c | 20.5 b | 25.1 a | 24.5 a | |
| $D_{P3}$ (*td*) | | | | | | | |
| SH | 16.5 | 13.2 | 20.7 | 28.1 | 12.9 | 14.1 | 17.6 bc |
| RH | 15.1 | 15.3 | 23.9 | 22.7 | 9.5 | 19.2 | 17.6 bc |
| Première | 8.7 | 17.2 | 22.4 | 13.1 | 16.7 | 12.4 | 15.1 c |
| Bintje | 27.1 | 24.2 | 34.7 | 19.4 | 13.0 | 16.1 | 22.4 b |
| Seresta | 17.6 | 24.7 | 28.9 | 10.9 | 8.5 | 16.4 | 17.8 bc |
| Astarte | 37.4 | 41.5 | 9.1 | 10.3 | 8.8 | 13.1 | 20.0 bc |
| Karnico | 51.3 | 54.0 | 12.5 | 18.1 | – | – | 34.0 a |
| Mean [2] | 24.8 b | 27.1 a | 21.7 c | 17.5 d | 11.6 f | 15.2 e | |
| F1 mean [3] | 16.5 d | 19.4 b | 24.3 a | 17.9 c | 16.0 d | 16.3 d | |
| $A_{sum}$ (*% td*) | | | | | | | |
| SH | 3713 | 3457 | 3012 | 3853 | 4190 | 4015 | 3707 d |
| RH | 2715 | 2033 | 2046 | 3690 | 4552 | 3273 | 3051 e |
| Première | 3304 | 2681 | 2589 | 2979 | 4113 | 3948 | 3269 e |
| Bintje | 4412 | 3974 | 5224 | 4993 | 5104 | 4396 | 4684 c |
| Seresta | 5024 | 5273 | 5607 | 6168 | 6383 | 5647 | 5684 b |
| Astarte | 5215 | 5316 | 5778 | 6566 | 7188 | 6555 | 6103 a |
| Karnico | 5110 | 5095 | 7054 | 7568 | – | – | 6207 a |
| Mean [2] | 4213 e | 3976 f | 4473 d | 5116 b | 5255 a | 4639 c | |
| F1 mean [3] | 3455 d | 3332 e | 3094 f | 4138 c | 4685 a | 4246 b | |

Means followed by different letters are significantly different according to Fisher's Multiple Range Test ($P < 0.05$).
$t_e$ (*td*): LSD for genotype = 4.0; LSD for environment = 0.7; LSD for G × E = 6.9.
$v_{max}$ (%): LSD for genotype = 4.9; LSD for environment = 0.8; LSD for G × E = 8.5.
$D_{P1}$ (*td*): LSD for genotype = 3.0; LSD for environment = 0.5; LSD for G × E = 5.1.
$D_{P2}$ (*td*): LSD for genotype = 6.1; LSD for environment = 1.0; LSD for G × E = 10.6.
$D_{P3}$ (*td*): LSD for genotype = 6.6; LSD for environment = 1.1; LSD for G × E = 11.5.
$A_{sum}$ (*% td*): LSD for genotype = 386.4; LSD for environment = 64.1; LSD for G × E = 669.2.
[1] Genotype (two parents and four or five cultivars) mean across six experiments (i.e. environments).
[2] Mean of each individual environment across genotypes (two parents and four or five cultivars).
[3] F1 mean of each individual environment across F1 population (100 genotypes).

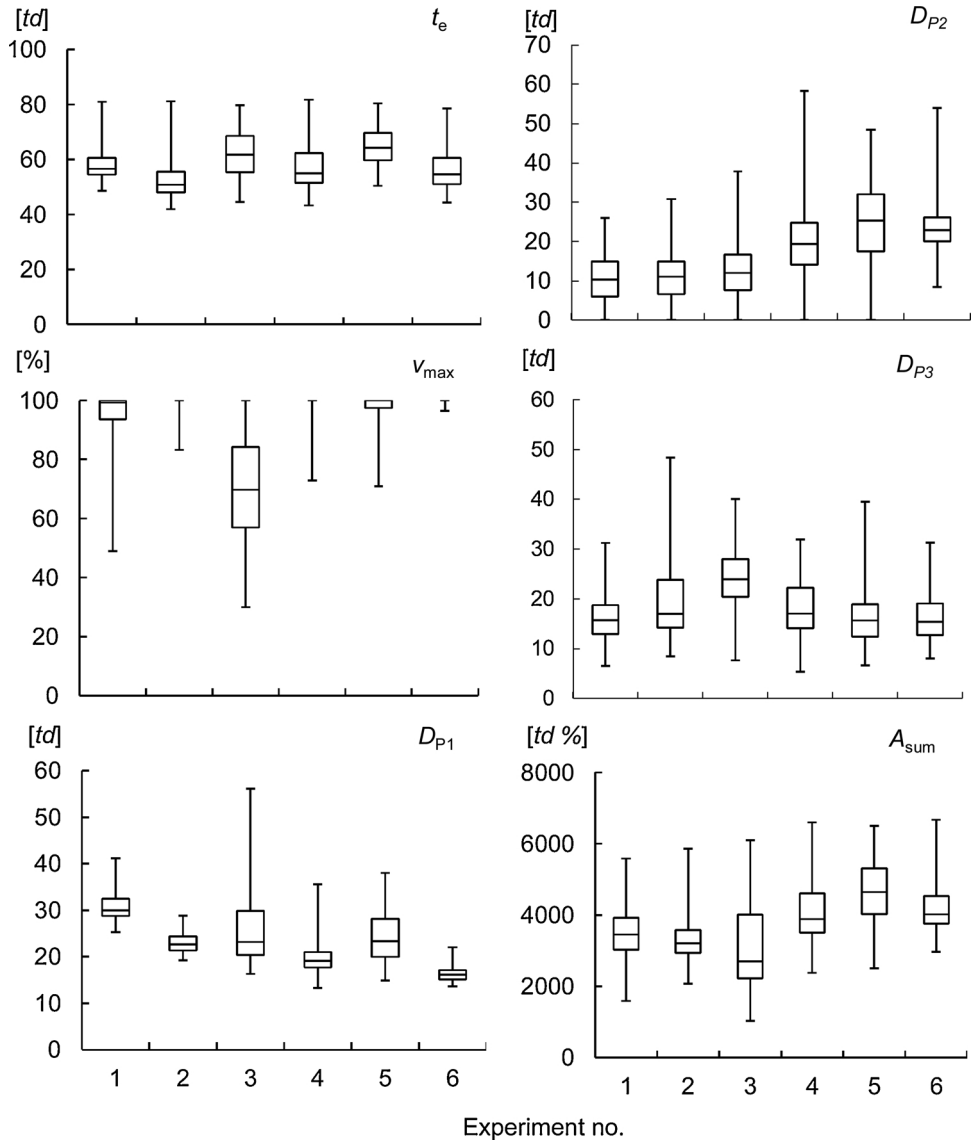


**Fig. 3.** Box plots of genetic means of an F1 population for model traits in all six experiments. The boxes span the interquartile range of the trait values, so that the middle 50% of the data lie within the box, with a horizontal line indicating the median. Whiskers extend beyond the ends of the box as far as the minimum and maximum values.

**Table 3**
Variance components for model traits within the F1 population across all six experiments.

| Parameter | $\sigma^2_{ph}$ | $\sigma^2_E$ | $\sigma^2_{\hat{\beta}}$ | $\sigma^2_G$ | $\sigma^2_{GE}$ | $\sigma^2_\varepsilon$ |
|---|---|---|---|---|---|---|
| $t_e$ (*td*) | 88.2 | 15.4** | 0.9** | 54.1** | 6.3** | 11.5 |
| $v_{max}$ (%) | 207.6 | 124.9** | 0.2NS | 16.9** | 45.7** | 19.9 |
| $D_{P1}$ (*td*) | 47.8 | 25.1** | 0.5** | 1.7** | 13.6** | 6.9 |
| $D_{P2}$ (*td*) | 128.5 | 44.3** | 2.2** | 33.5** | 19.9** | 28.6 |
| $D_{P3}$ (*td*) | 59.9 | 8.4* | 2.5** | 5.1** | 11.6** | 32.3 |
| $A_{sum}$ (% *td*) | 1206327 | 372964** | 9647** | 611003** | 99925** | 112788 |

$\sigma^2_{Ph}$ = phenotypic variance, $\sigma^2_{\hat{\beta}}$ = block variance, $\sigma^2_G$ = genetic variance, $\sigma^2_E$ = environmental variance, $\sigma^2_{GE}$ = genotype × environmental interaction variance, $\sigma^2_\varepsilon$ = residual variance.

** Significant at 1%.

* Significant at 5%.

NS Non-significant.

**Table 4**
The phenotypic coefficient of variation ($CV_{Ph}$%), genetic coefficient of variation ($CV_G$%), environmental coefficient of variation ($CV_E$%), and G × E interaction coefficient of variation ($CV_{GE}$%) for model traits within the F1 population across all six experiments.

| Parameter | Mean [1] | $CV_{Ph}$ | $CV_G$ | $CV_E$ | $CV_{GE}$ |
|---|---|---|---|---|---|
| $t_e$ (*td*) | 59.0 | 15.9 | 12.5 | 6.7 | 4.3 |
| $v_{max}$ (%) | 93.6 | 15.4 | 4.4 | 11.9 | 7.2 |
| $D_{P1}$ (*td*) | 23.3 | 29.7 | 5.6 | 21.5 | 15.8 |
| $D_{P2}$ (*td*) | 17.4 | 65.1 | 33.3 | 38.3 | 25.6 |
| $D_{P3}$ (*td*) | 18.4 | 42.1 | 12.3 | 15.8 | 18.5 |
| $A_{sum}$ (% *td*) | 3801 | 28.9 | 20.6 | 16.1 | 8.3 |

[1] Grand mean of the F1 segregating population across all six experiments.

**Table 5**
Phenotypic (lower triangle) and genetic (upper triangle) correlation coefficients among all pair-wise comparisons of model traits within the F1 population per individual experiment. The unit for all model traits is thermal day (*td*) except for $v_{max}$ (%) and the $A_{sum}$ (% *td*).

| | $t_e$ | $v_{max}$ | $D_{P1}$ | $D_{P2}$ | $D_{P3}$ | $A_{sum}$ |
|---|---|---|---|---|---|---|
| ***Exp. 1*** | | | | | | |
| $t_e$ | – | 0.37** | −0.41** | 0.72** | 0.78** | 0.88** |
| $v_{max}$ | 0.32** | – | −0.60** | 0.60** | 0.15NS | 0.73** |
| $D_{P1}$ | −0.38** | −0.48** | – | −0.82** | −0.20* | −0.70** |
| $D_{P2}$ | 0.64** | 0.51** | −0.75** | – | 0.24* | 0.90** |
| $D_{P3}$ | 0.70** | 0.09NS | −0.21* | 0.03NS | – | 0.55** |
| $A_{sum}$ | 0.85** | 0.70** | −0.62** | 0.84** | 0.43** | – |
| ***Exp. 2*** | | | | | | |
| $t_e$ | – | 0.46** | −0.43** | 0.67** | 0.84** | 0.97** |
| $v_{max}$ | 0.25* | – | −0.78** | 0.69** | 0.25** | 0.60** |
| $D_{P1}$ | −0.31** | −0.34** | – | −0.42** | −0.46** | −0.51** |
| $D_{P2}$ | 0.52** | 0.30** | −0.45** | – | 0.19NS | 0.82** |
| $D_{P3}$ | 0.78** | 0.13NS | −0.27** | −0.09NS | – | 0.71** |
| $A_{sum}$ | 0.95** | 0.37** | −0.43** | 0.74** | 0.58** | – |
| ***Exp. 3*** | | | | | | |
| $t_e$ | – | 0.75** | 0.77** | 0.66** | −0.13NS | 0.91** |
| $v_{max}$ | 0.69** | – | 0.88** | 0.16NS | −0.23* | 0.94** |
| $D_{P1}$ | 0.69** | 0.79** | – | 0.15NS | −0.42** | 0.88** |
| $D_{P2}$ | 0.42** | 0.17NS | −0.03NS | – | −0.21* | 0.46** |
| $D_{P3}$ | 0.00NS | −0.22* | −0.24* | −0.59** | – | −0.31** |
| $A_{sum}$ | 0.87** | 0.93** | 0.78** | 0.43** | −0.29** | – |
| ***Exp. 4*** | | | | | | |
| $t_e$ | – | 0.32** | −0.54** | 0.91** | 0.46** | 0.98** |
| $v_{max}$ | 0.21* | – | −0.62** | 0.59** | −0.30** | 0.51** |
| $D_{P1}$ | −0.37** | −0.34** | – | −0.70** | −0.19* | −0.64** |
| $D_{P2}$ | 0.82** | 0.36** | −0.59** | – | 0.09NS | 0.98** |
| $D_{P3}$ | 0.39** | −0.12NS | −0.14NS | −0.13NS | – | 0.29** |
| $A_{sum}$ | 0.96** | 0.40** | −0.45** | 0.92** | 0.17NS | – |
| ***Exp. 5*** | | | | | | |
| $t_e$ | – | 0.48** | 0.05NS | 0.80** | −0.60** | 0.93** |
| $v_{max}$ | 0.29** | – | −0.65** | 0.94** | −1.00** | 0.77** |
| $D_{P1}$ | 0.00NS | −0.36** | – | −0.53** | 0.30** | −0.26** |
| $D_{P2}$ | 0.71** | 0.57** | −0.52** | – | −0.79** | 0.97** |
| $D_{P3}$ | −0.11NS | −0.44** | 0.07NS | −0.59** | – | −0.85** |
| $A_{sum}$ | 0.89** | 0.62** | −0.26** | 0.91** | −0.42** | – |
| ***Exp. 6*** | | | | | | |
| $t_e$ | – | 0.00NS | 0.24* | 0.84** | 0.58** | 0.98** |
| $v_{max}$ | 0.15NS | – | 0.00NS | 0.00NS | 0.00NS | 0.00NS |
| $D_{P1}$ | 0.16NS | −0.25** | – | −0.24** | 0.66** | 0.07NS |
| $D_{P2}$ | 0.75** | 0.24* | −0.20* | – | 0.06NS | 0.92** |
| $D_{P3}$ | 0.49** | −0.03NS | 0.23* | −0.18NS | – | 0.43** |
| $A_{sum}$ | 0.97** | 0.22* | 0.03NS | 0.88** | 0.28** | – |

** Significant at 1%.
* Significant at 5%.
NS Non-significant.

**Table 6**
Broad-sense heritability $H^2$ (%) estimates across six experiments (Eq. 8) and per individual experiment (Eq. 9) for model traits within the F1 population per individual experiment.

| Parameter | $H^2$ [1] | Exp. 1 | Exp. 2 | Exp. 3 | Exp. 4 | Exp. 5 | Exp. 6 |
|---|---|---|---|---|---|---|---|
| $t_e$ (*td*) | 96.4 | 89.2 | 92.1 | 92.8 | 92.0 | 85.8 | 89.4 |
| $v_{max}$ (%) | 64.6 | 88.2 | 22.9 | 92.6 | 56.5 | 46.1 | 0.0 |
| $D_{P1}$ (*td*) | 37.4 | 79.9 | 55.7 | 89.2 | 69.5 | 77.6 | 75.6 |
| $D_{P2}$ (*td*) | 85.5 | 82.6 | 64.4 | 54.5 | 88.6 | 80.8 | 81.2 |
| $D_{P3}$ (*td*) | 52.4 | 60.6 | 73.3 | 30.0 | 51.3 | 23.3 | 39.6 |
| $A_{sum}$ (% *td*) | 95.9 | 92.3 | 90.6 | 94.9 | 94.0 | 88.1 | 92.6 |

[1] Broad-sense heritability across six environments.

also showed strong positive genetic correlations between $D_{P3}$ and $t_e$. These results indicate that genotypes with longer $D_{P2}$ and $D_{P3}$ could be indirectly obtained by selecting genotypes with high $v_{max}$ and $t_e$. The results revealed strong positive genetic correlations of traits ($t_e$, $v_{max}$, $D_{P2}$) with $A_{sum}$ in almost all experiments.

### 3.5. Estimates of broad-sense heritability

The estimates of broad-sense heritability ($H^2$) across six environments (Eq. (8)) varied greatly with traits under investigation (Table 6). The heritability values ranged from 37.4% to 96.4%. High estimates ($H^2 > 70\%$) were recorded for $t_e$, $D_{P2}$, and $A_{sum}$. Moderate estimates ($50\% < H^2 < 70\%$) were recorded for $v_{max}$ and $D_{P3}$ (Table 6). On the other hand, $D_{P1}$ had a weak heritability (37.4%). Table 6 also presents the estimates of broad-sense heritability ($H^2$) per individual experiment (Eq. (9)), which, in principle, should be higher than the estimates across environments, because for individual environments the genetic and G × E interaction effects are less confounded.

### 3.6. Genetic mapping

Among a total of 566 markers, 325 segregated due to polymorphism in the maternal (SH) parent < ab × aa > , while 241 segregated from the paternal (RH) parent < aa × ab > . Out of 566 markers, a total of 407 markers were mapped and the total data set was split into maternal (SH) and paternal (RH) data sets. Lack of sufficient bridging markers prevented making an integrated map.

The maternal data set could be split into 12 linkage groups at a recombination frequency threshold of 0.25. Twelve parent-specific linkage groups were obtained for both SH and RH (Supplementary Figs S1 and S2). However, linkage group I was divided into two subgroups (denoted as IA and IB, respectively) in the paternal (RH) map due to a lack of a sufficient number of in-between markers. Ninety-five of the 325 AFLP SH markers could not be assigned to the SH linkage groups. In the case of RH markers, 64 out of 241 markers could not be assigned to the RH linkage groups. The number of AFLP markers finally retained in the maternal and paternal maps were therefore 230 and 177, respectively, covering the genome size of 1902.9 cM.

The length of the linkage groups in the SH parental map ranged from 35.7 to 129.3 cM with a median distance of 2.0 cM between the loci. The RH parental map ranged from 28.0 to 101.1 cM and the median distance between loci was 2.5 cM. In both parental maps, the largest gap between loci was on linkage group X of 10.5 cM and 14.1 cM in SH and RH, respectively.

### 3.7. QTL detection

QTL analysis for model traits was conducted separately for the six environments (i.e. experiments). In total 25 QTLs were identified for our selected model traits on both SH and RH parental genomes across all six environments (Table 7; Supplementary Figs S1 and S2). In the SH genome, 15 QTLs were associated with six linkage groups (I, IV, V, VI, VIII, and XI). Twelve QTLs were shared by the RH genome on five linkage groups (I, II, IV, V and VI).

Table 7 summarises the list of QTLs detected, their parental chromosomes and map positions and their characteristics (i.e. additive effects and variance explained ($R^2$) for each of the trait investigated for individual environments). All the QTLs detected were significant at ($P < 0.05$) with $-\log_{10}(P)$ values ranging from 3.37 to 52.33. The total fraction of phenotypic variance explained by effects of each QTL were moderate (ranging from < 0.1% to 74%), but a high percentage of phenotypic variance was accounted for when considering the global $R^2$ (ranging from 28% to 82%) (Table 7).

Results indicated that QTLs with major effects were associated with paternal (RH) linkage groups, especially RH V, where in total two major QTLs were detected (Table 7). QTLs on this linkage group had negative additive effects, indicating that RH alleles on this linkage group share an antagonistic effect on the physiological traits related with canopy cover. One particular QTL (116_5_17) on this linkage group was detected for all model traits with a major additive effect and explained most of the total phenotypic variance (Fig. S2). Large number of additional QTLs with minor effects was mostly associated with maternal

**Table 7**
Main characteristics of quantitative trait loci (QTL) identified for model traits within the 'SH × RH' population per individual experiment (i.e. environment.). Data given in table are from the CIM mapping method. QTLs marked as bold are detected only by the CIM method, otherwise by both the CIM and SIM methods. Exp., experiment; position, position of maximum –$\log_{10}$ ($P$); a, additive effect of the presence of parental allele at a marker; $R^2$, the individual contribution of one QTL to the variation in a trait; global $R^2$, the fraction of the total variation explained by QTLs of the same trait within single environment; *td*, thermal day. Symbol '–' means no QTL was detected.

| Parameter | Exp. | QTL | Linkage group | Marker name | Position (cM) | -$\log_{10}(P)$ | a | $R^2$ | Global $R^2$ |
|---|---|---|---|---|---|---|---|---|---|
| $t_e$ (*td*) | 1 | 116_5_17 | RH V | EAGAMCTC_470_5_17 | 18.2 | 19.50 | −19.351 | 0.51 | |
| | 2 | 116_5_17 | RH V | EAGAMCTC_470_5_17 | 18.2 | 24.25 | −27.232 | 0.55 | 0.62 |
| | | **108_4_72** | **RH IV** | **EAACMCCA_92.1_4_72** | **46.9** | 3.93 | 8.408 | 0.02 | |
| | 3 | 116_5_17 | RH V | EAGAMCTC_470_5_17 | 18.2 | 26.91 | −29.497 | 0.58 | 0.68 |
| | | **101_4_35** | **RH IV** | **EAGAMCAG_216.2_4_35** | **9.6** | 3.95 | 7.580 | 0.03 | |
| | | **153_6_28** | **RH VI** | **PAT/MAAC_272.6_6_28** | **53.8** | 3.62 | 7.112 | 0.02 | |
| | 4 | 116_5_17 | RH V | EAGAMCTC_470_5_17 | 18.2 | 20.612 | −32.356 | 0.65 | |
| | 5 | 116_5_17 | RH V | EAGAMCTC_470_5_17 | 18.2 | 19.527 | −24.133 | 0.63 | |
| | 6 | 116_5_17 | RH V | EAGAMCTC_470_5_17 | 18.2 | 52.33 | −49.912 | 0.74 | |
| $v_{max}$ (%) | 1 | 170_5_44 | SH V | PAC/MAAC_190.2_5_44 | 26.8 | 5.66 | 22.660 | 0.21 | |
| | 2 | – | – | – | – | – | – | – | |
| | 3 | 116_5_17 | RH V | EAGAMCTC_470_5_17 | 18.2 | 26.28 | −54.862 | 0.56 | 0.65 |
| | | **21_1_32** | **SH I** | **EACAMCAG_381.9_1_32** | **38.7** | 3.80 | 4.243 | 0.02 | |
| | | **63_1_42** | **SH I** | **PAG/MACC_322.2_1_42** | **69.0** | 4.78 | 16.533 | 0.12 | |
| | 4 | 170_5_44 | SH V | PAC/MAAC_190.2_5_44 | 26.8 | 4.291 | 8.836 | 0.18 | |
| | 5 | – | – | – | – | – | – | – | |
| | 6 | – | – | – | – | – | – | – | |
| $D_{P1}$ (*td*) | 1 | 116_5_17 | RH V | EAGAMCTC_470_5_17 | 18.2 | 6.23 | 7.404 | 0.23 | |
| | 2 | 98_4_35 | RH IV | EACAMCTG_138.9_4_35 | 12.8 | 3.48 | 3.167 | 0.13 | |
| | 3 | 116_5_17 | RH V | EAGAMCTC_470_5_17 | 18.2 | 18.02 | −26.586 | 0.60 | |
| | 4 | 63_1_42 | SH I | PAG/MACC_322.2_1_42 | 69.0 | 4.738 | −5.754 | 0.17 | 0.28 |
| | | **96_4_33** | **RH IV** | **EACAMCAC_156.4_4_33** | **5.5** | 3.423 | 4.691 | 0.11 | |
| | 5 | – | – | – | – | – | – | – | |
| | 6 | 291_11_7 | SH XI | EACAMCAC_372_11_7 | 9.2 | 3.371 | −2.591 | 0.14 | |
| $D_{P2}$ (*td*) | 1 | 116_5_17 | RHV | EAGAMCTC_470_5_17 | 18.2 | 11.48 | −16.987 | 0.37 | |
| | 2 | **133_4_28** | **SH IV** | **EACTMCTG_74.3_4_28** | **24.8** | 4.09 | 6.655 | 0.09 | 0.35 |
| | | 200_6_56 | SH VI | PAT/MAAC_155.4_6_56 | 73.5 | 4.30 | 6.996 | 0.13 | |
| | | 116_5_17 | RH V | EAGAMCTC_470_5_17 | 18.2 | 4.08 | −10.208 | 0.14 | |
| | 3 | – | – | – | – | – | – | – | |
| | 4 | 116_5_17 | RH V | EAGAMCTC_470_5_17 | 18.2 | 26.28 | −30.089 | 0.56 | 0.70 |
| | | **14_1_30** | **SH I** | **EAGTMCAG_458_1_30** | **33.1** | 6.82 | 2.830 | 0.03 | |
| | | **62_1_36** | **SH I** | **EAGAMCAG_228.3_1_36** | **64.0** | 8.39 | 9.433 | 0.15 | |
| | | **76_1_84** | **SH I** | **PAT/MAAC_259.4_1_84** | **110** | 4.15 | 4.610 | 0.02 | |
| | 5 | 116_5_17 | RH V | EAGAMCTC_470_5_17 | 18.2 | 11.983 | −31.322 | 0.45 | |
| | 6 | 116_5_17 | RH V | EAGAMCTC_470_5_17 | 18.2 | 8.355 | −17.625 | 0.22 | 0.38 |
| | | **47_1_63** | **RH IB** | **EACAMCCT_144.5_1_63** | **27.8** | 4.686 | 11.283 | 0.04 | |
| $D_{P3}$ (*td*) | 1 | 116_5_17 | RH V | EAGAMCTC_470_5_17 | 18.2 | 5.26 | −9.768 | 0.20 | |
| | 2 | 116_5_17 | RH V | EAGAMCTC_470_5_17 | 18.2 | 14.39 | −19.569 | 0.42 | |
| | 3 | – | – | – | – | – | – | – | |
| | 4 | – | – | – | – | – | – | – | |
| | 5 | 39_1_32 | SH I | EAACMCCT_217.8_1_32 | 41.6 | 4.101 | −8.657 | 0.17 | |
| | 6 | **1_5_12** | **SH V** | **SH05B012_maturity_locus** | **0.0** | 4.573 | −8.988 | 0.08 | 0.46 |
| | | **242_8_29** | **SH VIII** | **PAT/MAAC_283.7_8_29** | **33.2** | 4.134 | −6.785 | 0.08 | |
| | | 115_5_4 | RH V | PAC/MAGT_190.2_5_4 | 1.6 | 9.326 | −12.803 | 0.24 | |
| $A_{sum}$ (% *td*) | 1 | 116_5_17 | RH V | EAGAMCTC_470_5_17 | 18.2 | 19.65 | −2359.408 | 0.50 | 0.57 |
| | | 43_1_35 | RH IA | PAT/MAGT_143.9_1_35 | 58.3 | 3.60 | 786.981 | < 0.1 | |
| | 2 | 116_5_17 | RH V | EAGAMCTC_470_5_17 | 18.2 | 21.09 | −2188.154 | 0.52 | 0.59 |
| | | **199_6_48** | **SH VI** | **EACAMCCT_138.9_6_48** | **61.8** | 3.91 | 719.654 | 0.03 | |
| | 3 | 116_5_17 | RH V | EAGAMCTC_470_5_17 | 18.2 | 28.68 | −4112.081 | 0.69 | 0.82 |
| | | **63_1_42** | **SH I** | **PAG/MACC_322.2_1_42** | **69.0** | 3.953 | 878.855 | 0.07 | |
| | | **179_5_77** | **SH V** | **PAC/MATA_201.4_5_77** | **77.2** | 4.883 | 974.202 | < 0.1 | |
| | | **81_2_75** | **RH II** | **PAC/MAGG_527.2_2_75** | **79.1** | 4.481 | −938.074 | < 0.1 | |
| | 4 | 116_5_17 | RH V | EAGAMCTC_470_5_17 | 18.2 | 40.06 | −2996.801 | 0.67 | 0.73 |
| | | **66_1_52** | **SH I** | **EAACMCTG_193.9_1_52** | **81.5** | 4.11 | 419.656 | 0.06 | |
| | | **39_1_32** | **SH I** | **EAACMCCT_217.8_1_32** | **41.6** | 4.51 | 552.856 | 0.08 | |
| | 5 | 116_5_17 | RH V | EAGAMCTC_470_5_17 | 18.2 | 29.21 | −2991.844 | 0.59 | 0.65 |
| | | **79_2_72** | **RH II** | **EACTMCTC_444.3_2_72** | **73.8** | 3.70 | −815.825 | < 0.1 | |
| | 6 | 116_5_17 | RH V | EAGAMCTC_470_5_17 | 18.2 | 18.77 | −2185.245 | 0.49 | |

(SH) linkage groups (Table 8). A QTL with main effect was found on chromosome V. We also observed the co-localisation of QTLs for many traits. For instance, clustering of many QTLs were found on position 18.2 cM on paternal (RH) linkage group (Table 9). Here most of the traits (e.g. $D_{P2}$, $A_{sum}$) were tightly linked with QTL (116_5_17) in most of the environments. This could mean that this QTL is playing a pleiotropic role in determining these traits.

For model traits ($v_{max}$, $D_{P1}$, and $D_{P3}$), some QTLs identified were expressed in one environment but not in the other ones thereby exhibiting QTL × E (Table 7). For all these traits the G × E component of phenotypic variance was greater than the G variance component (Table 3).

## 4. Discussion

### 4.1. Model performance

Our analyses showed that the model for canopy cover (Fig. 1 and

**Table 8**
List of parental linkage groups with major and additional minor QTLs.

| Parameter | SH linkage group | RH linkage group | |
|---|---|---|---|
| | Additional QTLs | Major QTL | Additional QTLs |
| $t_e$ | – | V | IV, VI |
| $v_{max}$ | I, V | V | – |
| $D_{P1}$ | I | V | IV |
| $D_{P2}$ | I, IV, VI | V | IB |
| $D_{P3}$ | I, V, VIII | V | – |
| $A_{sum}$ | I, V, VI | V | IA, II |

Eqs. (1–3)) performed very well for the canopy build-up phase and for the maximum canopy cover phase. It was possible to estimate important and agronomically relevant canopy parameters with a high accuracy and precision, for the standard cultivars, the parents and the F1 diploid population (Figs. 2–3). This high accuracy and precision made it possible to determine relevant genetic variation in canopy growth (Fig. 3). Most model traits (with the notable exception of $v_{max}$) were nearly normally distributed (Fig. 4). Parameters $t_e$, $D_{P2}$ and $A_{sum}$ were most important to describe the genetic variation in canopy cover.

However, the model did not perform very well for the canopy decline phase. Data for this phase were sometimes scarce for late genotypes, because of the late onset of senescence. Moreover, data for this period also showed more variation, as the sagging of the canopy resulted in an irregular spatial distribution of the remaining green leaves. It was therefore not possible to estimate the moment of fastest canopy decline, which could have been a valuable additional parameter similar to $t_{m1}$. Nevertheless, the combined Eqs. (1–3) could be very useful in analysing the canopy cover dynamics of a diverse set of potato genotypes under various environments and making inferences about the underlying processes controlling canopy growth.

### 4.2. Impact of environment on model parameters

Environment had a highly significant ($P < 0.01$) impact on all model traits (Table 2), at least partly due to the purposeful variation in availability of N across trials (Table 1). Nitrogen has a main influence on canopy development (Perumal and Sahota, 1986; Vos, 1995a, b, 2009), arising from effects of N on rate and duration of appearance of leaves and branches on the potato plant, and on the active life span of individual leaves. Due to the lack of precise information about amount of mineral N becoming available during the course of canopy growth, we used the amount of N uptake by tubers as an indicator of N availability (Table 1). Crop N uptake is a site-specific indicator of N that is "available" to the crop (Sullivan et al., 2008). Experiments with lower N uptake (especially Exp. 3) had lower estimates for $v_{max}$, $D_{P2}$ and $A_{sum}$. In potato, the duration of *P*2 and whether or not full canopy cover is attained are very much affected by N supply. The total growth period is prolonged for larger rate of N supply because *P*2 extends with better N nutrition (Ospina et al., 2014). Usually, within agronomically relevant ranges, N has comparatively little effect on *P*1 and affects the rate of senescence only marginally (Vos, 2009), although Ospina et al. (2014) observed that the *DP*1 was longer under low N. In our most extreme experiment (Exp. 3), we also found a long *DP*1 and a high $t_e$ in comparison with environments with higher N availability (high tuber N uptake) (Tables 1 and 2).

### 4.3. Model restrictions

The canopy build-up phase and the canopy decline phase are strongly influenced by the extent to which environmental conditions and maturity type will allow full canopy cover (Table 2). For example, low nitrogen supply or poor water availability can slow down the increase in $v$, limit $v_{max}$, limit the duration of the period during which $v_{max}$ is maintained and increase the rate with which $v$ is declining during the canopy decline phase. These effects can be stronger for early-

**Table 9**
List of co-localised [1] QTLs (listed under A) and independent [2] QTLs (listed under B), detected for model traits within F1 population per individual experiment.

| QTL | Linkage group | Position (cM) | Marker name | Exp. 1 | Exp. 2 | Exp. 3 | Exp. 4 | Exp. 5 | Exp. 6 |
|---|---|---|---|---|---|---|---|---|---|
| **A.** | | | | | | | | | |
| 39_1_32 | SH I | 41.6 | EAACMCCT_217.8_1_32 | | | | $A_{sum}$ | $D_{P3}$ | |
| 63_1_42 | SH I | 69.0 | PAG/MACC_322.2_1_42 | | | $v_{max}$, $A_{sum}$ | $D_{P1}$ | | |
| 116_5_17 | RH V | 18.2 | EAGAMCTC_470_5_17 | $t_e$, $D_{P1}$, $D_{P2}$, $D_{P3}$, $A_{sum}$ | $t_e$, $D_{P2}$, $D_{P3}$, $A_{sum}$ | $t_e$, $v_{max}$, $D_{P1}$, $A_{sum}$ | $t_e$, $D_{P2}$, $A_{sum}$ | $t_e$, $D_{P2}$, $A_{sum}$ | $t_e$, $D_{P2}$, $A_{sum}$ |
| **B.** | | | | | | | | | |
| 14_1_30 | SHI | 33.1 | EAGTMCAG_458_1_30 | | | | $D_{P2}$ | | |
| 21_1_32 | SHI | 38.7 | EACAMCAG_381.9_1_32 | | | $v_{max}$ | | | |
| 62_1_36 | SH I | 64.0 | EAGAMCAG_228.3_1_36 | | | | $D_{P2}$ | | |
| 66_1_52 | SH I | 81.5 | EAACMCTG_193.9_1_52 | | | | $A_{sum}$ | | |
| 76_1_84 | SH I | 110.0 | PAT/MAAC_259.4_1_84 | | | | $D_{P2}$ | | |
| 133_4_28 | SH IV | 24.8 | EACTMCTG_74.3_4_28 | | $D_{P2}$ | | | | |
| 1_5_12 | SH V | 0.0 | SH05B012_maturity_locus | | | | | | $D_{P3}$ |
| 179_5_77 | SH V | 77.2 | PAC/MATA_201.4_5_77 | | | $A_{sum}$ | | | |
| 199_6_48 | SH VI | 61.8 | EACAMCCT_138.9_6_48 | | $A_{sum}$ | | | | |
| 200_6_56 | SH VI | 73.5 | PAT/MAAC_155.4_6_56 | | | $D_{P2}$ | | | |
| 242_8_29 | SH VIII | 33.2 | PAT/MAAC_283.7_8_29 | | | | | | $D_{P3}$ |
| 291_11_7 | SH XI | 9.2 | EACAMCAC_372_11_7 | | | | | | $D_{P1}$ |
| 43_1_35 | RH IA | 58.3 | PAT/MAGT_143.9_1_35 | $A_{sum}$ | | | | | |
| 47_1_63 | RH IB | 27.8 | EACAMCCT_144.5_1_63 | | | | | | $D_{P2}$ |
| 79_2_72 | RH II | 73.8 | EACTMCTC_444.3_2_72 | | | | | $A_{sum}$ | |
| 81_2_75 | RH II | 79.1 | PAC/MAGG_527.2_2_75 | | | $A_{sum}$ | | | |
| 96_4_33 | RH IV | 5.5 | EACAMCAC_156.4_4_33 | | | | $D_{P1}$ | | |
| 101_4_35 | RH IV | 9.6 | EAGAMCAG_216.2_4_35 | | | $t_e$ | | | |
| 98_4_35 | RH IV | 12.8 | EACAMCTG_138.9_4_35 | | $D_{P1}$ | | | | |
| 108_4_72 | RH IV | 46.9 | EAACMCCA_92.1_4_72 | | $t_e$ | | | | |
| 115_5_4 | RH V | 1.6 | PAC/MAGT_190.2_5_4 | | | | | | $D_{P3}$ |
| 153_6_28 | RH VI | 53.8 | PAT/MAAC_272.6_6_28 | | | $t_e$ | | | |

[1] QTL is similar for more than one trait.
[2] QTL is different for a particular trait in any experiment (environment).

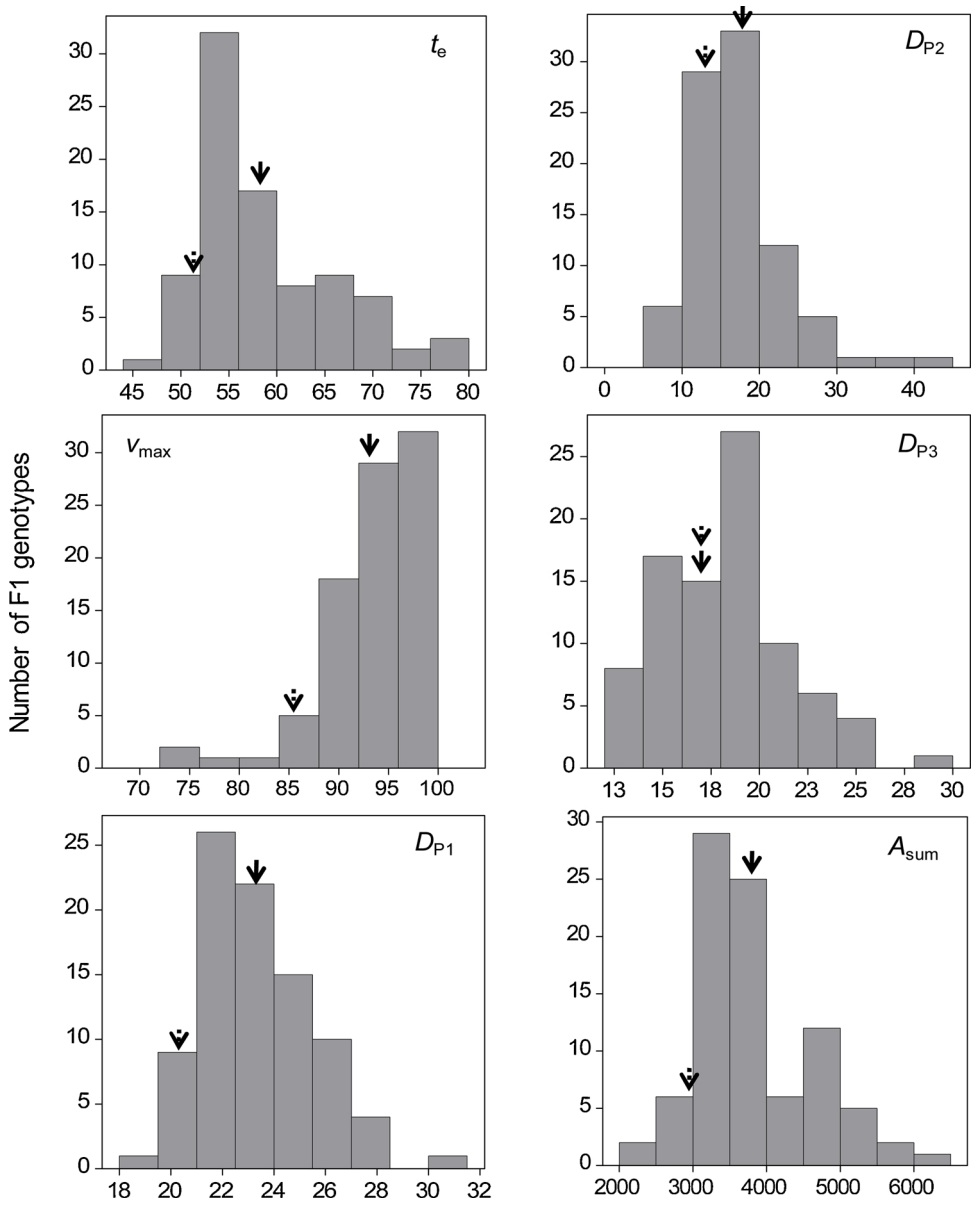


**Fig. 4.** Distribution of model traits among F1 genotypes across six experiments. The values of two parents 'SH' and 'RH' are indicated by full arrow and dashed arrow, respectively. Values on the X-axes represent *td* (thermal days) for $t_e$, $D_{P1}$, $D_{P2}$, $D_{P3}$, % for $v_{max}$, and *td* % for $A_{sum}$. Values on Y-axes indicate number of F1 genotypes.

maturing types than for late-maturing types (Fig. 2). Such conditions might cause a delay of $t_{m1}$, $t_1$ and $t_e$, but can advance $t_2$ (Fig. 2). They will also create a more pronounced maximum value of $v_{max}$ which will not last long. The estimate of $v_{max}$ might still be accurate but $D_{P2}$ will be short and less precisely predicted by the model.

Canopy growth can be irregular when temporary drought is followed by restored water availability or when secondary growth occurs associated with a period of warm weather. Such development of canopy cover cannot be covered by the current equations. In growing seasons with extreme weather conditions, we have observed a temporary halting of the increase of *v*. Such a period could be followed by a new period of increase in *v* when conditions for vegetative growth improve. Our models will not capture that type of crop behaviour. It would also be impossible under such conditions to estimate the duration of the maximum canopy cover phase. Fortunately, such growing seasons are relatively rare and did not occur during the field experimentation described in this paper.

Our way of assessing canopy cover provides a proxy for the development over time of light interception and for the leaf area index. However, it does not reflect the changes in leaf area index during the

**Table 10**
List of stable QTLs across six experiments (i.e. similar QTLs detected in several environments).

| QTL | Group | Position (cM) | Marker name | Exp. 1 | Exp. 2 | Exp. 3 | Exp. 4 | Exp. 5 | Exp. 6 |
|---|---|---|---|---|---|---|---|---|---|
| 39_1_32 | SH I | 41.6 | EAACMCCT_217.8_1_32 | | | | × | × | |
| 63_1_42 | SH I | 69.0 | PAG/MACC_322.2_1_42 | | | × | × | | |
| 170_5_44 | SH V | 26.6 | PAC/MAAC_190.2_5_44 | × | | | × | | |
| 116_5_17 | RH V | 18.2 | EAGAMCTC_470_5_17 | × | × | × | × | × | × |

maximum canopy cover phase. If $\nu_{max}$ is 100%, variation in leaf area index during $D_{P2}$ can be considerable and LAI can easily range from 3 to 6 or even more. If $\nu_{max}$ remains below 100%, the canopy cover development will reflect the development of LAI across the entire crop cycle.

Boyd et al. (2002) analysed the relation between LAI and canopy cover and showed that the slope of this relationship depended on crop management. However, they also showed that ground cover duration explained variation in tuber yield equally well as, or even better than, leaf area duration.

### 4.4. Genetic aspects of canopy cover

The environmental and genetic variances of model traits were always significant (Table 3). The $CV_{GE}$ was larger than the $CV_G$ and $CV_E$ for $D_{P3}$, while the $CV_G$ was larger than the $CV_E$ for $t_e$ and $A_{sum}$ (Table 4). The phenotypic and genetic correlations were higher for $D_{P1}$ versus $D_{P2}$ than for $D_{P2}$ versus $D_{P3}$ in Experiments 1, 2, 4, and 6, but the opposite was true in Experiments 3 and 5 (Table 5). The correlation coefficients between $A_{sum}$ and $t_e$ or $D_{P2}$ were highest in all experiments except for Experiments 3 and 5. These results underline the importance of the genetic variation in maturity type as illustrated by genetic variation in $t_e$ and $A_{sum}$ and the complexity and relatively poor repeatability of the canopy decline phase. They also stress the different nature of the data sets of Experiments 3 and 5 due to the relatively high heritability of $\nu_{max}$ (Experiment 3) and/or low heritability of $D_{P3}$ (Experiments 3 and 5).

High genetic correlations between model traits (Table 5) suggest that genetically manipulating various traits simultaneously might not be easy. Pleiotropy might be a common phenomenon for some of our model traits. Pleiotropy can have important implications for our understanding of the nature of genetic correlations between different traits in certain regions of a genome and also for practical applications in breeding because one of the major goals in breeding is to break unfavourable linkage (Jiang and Zeng, 1995).

The high heritability estimates across the six environments (Table 6) showed that most traits varied consistently under contrasting environmental conditions. $D_{P1}$ was an exception. Heritability estimates per environment were high but in some experiments heritability estimates were rather low for $\nu_{max}$ and $D_{P3}$. However, only few QTLs were stable across the environments and therefore only a few did not show much QTL × E (Tables 7, 8, and 9). For instance, the QTL 116_5_17 on RH V showed up in all the experiments for $A_{sum}$ (Table 10; Fig. S2). Such QTLs could be useful for marker assisted breeding.

Our linkage map was generally consistent with the ultra-dense map described by Van Os et al. (2006). However, the SH linkage groups VIII and X were 37% and RH linkage group VII was 29% shorter than in the ultra-dense map of Van Os et al. (2006). These differences were due to differences in the size of the SH × RH mapping populations used.

Linkage group V harbours the QTL for plant maturity and vigour in potato (Collins et al., 1999; Oberhagemann et al., 1999; Visker et al., 2003; Bradshaw et al., 2008). Our results also confirm this fact as most of our canopy growth and development traits (particularly $A_{sum}$) could be very useful in defining the maturity type in potato (cf. Khan et al., 2013). Our results demonstrate that maturity in potato was mainly expressed from the paternal (RH) side. We also found a large number of independent QTLs (i.e. they did not coincide with other traits) (Table 9).

### 4.5. Relation between canopy cover and biomass accumulation and tuber yield

Model traits $t_e$, $A_{sum}$ and $D_{P2}$ showed the highest values for broad sense heritability across environments (Table 6). These traits are associated with the duration of maximum canopy cover and therefore with the amount of light intercepted and the amount of biomass produced by the crop. The total biomass production and accumulation of potato cultivars are dependent on the intercepted PAR (Spitters, 1988; Vos and Groenwold, 1989; Van Delden et al., 2001). The amount of light intercepted is in proportion to the area under the whole green canopy curve (Vos, 1995b). Kooman and Rabbinge (1996) found that, compared with late cultivars, early potato cultivars allocate a larger part of the available assimilates to the tubers early in the growing season, resulting in shorter growing periods and also lower yields. This shows that late genotypes may have higher potential to intercept the PAR and tuber yield production under both resource (N) optimum and – poor growing conditions (Khan, 2012).

## 5. Conclusions

We presented a simple quantitative model which successfully described the quantitative differences in canopy dynamics of diverse genotypes in a segregating F1 population of potato under varied environments. It gave physiological insight using agronomically meaningful traits. These traits are directly related to the ability of the adapted genotypes to intercept photosynthetically active radiation and thus to create high tuber yields as we will show in the companion paper.

For most traits quantified in the model, high genetic variability along with high heritability were recorded within the F1 population under study. There are opportunities, therefore, to exploit the genetic variability available in the F1 population and to select for highly heritable traits in order to improve radiation interception efficiency.

We identified 28 QTLs on both SH and RH parental genomes across all six environments. QTLs with major effects were associated mainly with paternal (RH) linkage group V. One particular QTL (116_5_17) on this linkage group was detected for nearly all traits with a major additive effect and explained most of the total phenotypic variance. Some of the QTLs were mapped to similar positions in most environments. Only few QTLs were stable across environments.

Our quantitative approach in combination with markers of the widely available and easy-to-use AFLP marker system identified QTLs that could be useful in developing marker-assisted breeding strategies in potato.

## Ethics statement

The authors declare no conflict of interest.

## Acknowledgements

The authors gratefully acknowledge funding from the European Community under the Seventh Framework Programme for Research, Technological Development and Demonstration Activities, for the Integrated Project NUE-CROPS FP7-CP-IP 222645. The views expressed in this publication are the sole responsibility of the authors and do not necessarily reflect the views of the European Commission. Neither the European Commission nor any person acting on behalf of the Commission is responsible for the use which might be made of the information contained herein. M.S.K. was supported by a grant of the Higher Education Commission (HEC), Government of Pakistan. We are grateful to the assistance and support of the Netherlands Organization for International Cooperation in Higher Education (NUFFIC). We thank the UNIFARM staff of Wageningen University for their technical assistance.

## Appendix A. Supplementary data

Supplementary data associated with this article can be found, in the online version, at https://doi.org/10.1016/j.fcr.2019.107581.

## References


Allen, E.J., Scott, R.K., 1992. Principles of agronomy and their application in the potato industry. In: Harris, P.M. (Ed.), The Potato Crop: The Scientific Basis for Improvement. Chapman and Hall, London, UK, pp. 816–881.

Allen, E.J., Scott, R.K., 1980. An analysis of growth of the potato crop. J. Agric. Sci. 94, 583–606.

Almekinders, C.J.M., Struik, P.C., 1994. Photothermal response of sympodium development and flowering in potato (*Solanum tuberosum* L.) under controlled conditions. Neth. J. Agric. Sci. 42, 311–329.

Almekinders, C.J.M., Struik, P.C., 1996. Shoot development and flowering in potato (*Solanum tuberosum* L.). Potato Res. 39, 581–607.

Association of Official Analytical Chemistry (AOAC), 1984. Official Methods of Analysis of the Association of Official Analytical Chemists, 14th ed. Washington D.C., pp. 1141.

Boyd, N.S., Gordon, R., Martin, R.C., 2002. Relationship between leaf area index and ground cover in potato under different management conditions. Potato Res. 45, 117–129.

Bradshaw, J.E., 1994. Quantitative genetics theory for tetrasomic inheritance. In: Bradshaw, J.E., Mackay, G.R. (Eds.), Potato Genetics. CAB International, Wallingford, UK, pp. 71–99.

Bradshaw, J., Hackett, C., Pande, B., Waugh, R., Bryan, G., 2008. QTL mapping of yield, agronomic and quality traits in tetraploid potato (*Solanum tuberosum* subsp. *tuberosum*). Theor. Appl. Genet. 116, 193–211.

Burstall, L., Harris, P.M., 1983. The estimation of percentage light interception from leaf area index and percentage ground cover in potatoes. J. Agric. Sci. 100, 241–244.

Cadersa, Y., Govinde, N., 1999. Relationship between Canopy Cover and Light Interception in Potato in a Tropical Climate. Food and Agricultural Research Council, Réduit, Mauritius, pp. 137–144.

Chenu, K., Chapman, S.C., Tardieu, F., McLean, G., Welcker, C., Hammer, G.L., 2009. Simulating the yield impacts of organ-level quantitative trait loci associated with drought response in maize - a "gene-to-phenotype" modeling approach. Genetics 183, 1507–1523.

Collins, A., Milbourne, D., Ramsay, L., Meyer, R., Chatot-Balandras, C., Oberhagemann, P., de Jong, W., Gebhardt, C., Bonnel, E., Waugh, R., 1999. QTL for field resistance to late blight in potato are strongly correlated with earliness and vigour. Mol. Breed. 5, 387–398.

Daniell, H., Dhingra, A., 2002. Multigene engineering: dawn of an exciting new era in biotechnology. Curr. Opin. Biotechnol. 13, 136–141.

Ellis, R.H., Hadley, P., Roberts, E.H., Summerfield, R.J., 1990. Quantitative relations between temperature and crop development and growth. In: Jackson, M.T., Ford-Lloyd, B.V., Parry, M.L. (Eds.), Climatic Change and Plant Genetic Resources. Belhaven Press, London, pp. 85–115.

Fahem, M., Haverkort, A.J., 1988. Comparison of the growth of potato crops grown in autumn and spring in North Africa. Potato Res. 31, 557–568.

Falconer, D.S., Mackay, T.F.C., 1996. Introduction to Quantitative Genetics, fourth edition. Addison Wesley Longman, Harlow, Essex, UK.

Fernando, L.H., 1958. Studies on the Leaf Growth, Effect of Mineral Nutrients and the Interdependence of the Leaves of a Plant. PhD Thesis. University of London.

Firman, D.M., O'Brien, P.J., Allen, E.J., 1995. Appearance and growth of individual leaves in the canopies of several potato cultivars. J. Agric. Sci. 125, 379–394.

Fleisher, D.H., Timlin, D.J., 2006. Modeling expansion of individual leaves in the potato canopy. Agric. Forest. Meteorol. 139, 84–93.

Fleisher, D.H., Shillito, R.M., Timlin, D.J., Kim, S.-H., Reddy, V.R., 2006. Approaches to modeling potato leaf appearance rate. Agron. J. 98, 522–528.

Gutteling, E.W., Doroszuk, A., Riksen, J.A.G., Prokop, Z., Reszka, J., Kammenga, J.E., 2007. Environmental influence on the genetic correlations between life-history traits in *Caenorhabditis elegans*. Heredity 98, 206–213.

Hackett, C.A., Bradshaw, J.E., McNicol, J.W., 2001. Interval mapping of QTLs in autotetraploid species. Genetics 159, 1819–1832.

Hammer, G., Cooper, M., Tardieu, F., Welch, S., Walsh, B., Van Eeuwijk, F.A., Chapman, S., Podlich, D., 2006. Models for navigating biological complexity in breeding improved crop plants. Trends Plant. Sci. 11, 587–593.

Hammer, G.L., Van Oosterom, E., McLean, G., Chapman, S.C., Broad, I., Harland, P., Muchow, R.C., 2010. Adapting APSIM to model the physiology and genetics of complex adaptive traits in field crops. J. Exp. Bot. 61, 2185–2202.

Haverkort, A.J., Rutavisire, C., 1986. Fertilizer utilization under tropical conditions. 2. Effect of applying nitrogen, phosphorus and potassium on the relationship between intercepted radiation and yield of potatoes in central Africa. Potato Res. 29, 357–365.

Haverkort, A.J., Struik, P.C., 2015. Yield levels of potato crops: recent achievements and future prospects. Field Crops Res. 182, 76–85.

Hodges, T., 1991. Crop growth simulation and the role of phenological models. In: Hodges, T. (Ed.), Predicting Crop Phenology. CRC Press, Boston, pp. 3–5.

Holland, J.B., 2006. Estimating genotypic correlations and their standard errors using multivariate restricted maximum likelihood estimation with SAS proc mixed. Crop Sci. 46, 642–654.

Houle, D., 1992. Comparing evolvability and variability of quantitative traits. Genetics 130, 195–204.

Humphries, E.C., French, S.A.W., 1963. The effects of nitrogen, phosphorus, potassium and gibberellic acid on leaf area and cell division in Majestic potato. Ann. Appl. Biol. 52, 149–162.

Jansen, R.C., 1993. Interval mapping of multiple quantitative trait loci. Genetics 135, 205–211.

Jansen, R.C., 1995. Genetic Mapping Quantitative Trait Loci in Plants: a Novel Statistical Approach. PhD Dissertation. Wageningen University, The Netherlands.

Jansen, R.C., Stam, P., 1994. High resolution of quantitative traits into multiple loci via interval mapping. Genetics 136 1477–1455.

Jefferies, R.A., MacKerron, D.K.L., 1993. Responses of potato genotypes to drought. II. Leaf area index, growth and yield. Ann. Appl. Biol. 122, 105–112.

Jiang, C., Zeng, Z.-B., 1995. Multiple trait analysis of genetic mapping for quantitative trait loci. Genetics 140, 1111–1127.

Johnson, H.W., Robinson, H.F., Comstock, R.E., 1955. Genotype and phenotype correlations in soybeans and their implication in selection. Agron. J. 47, 477–483.

Khan, M.S., 2012. Assessing Genetic Variation in Growth and Development of Potato. PhD Thesis. Wageningen University, Wageningen.

Khan, M.S., van Eck, H.J., Struik, P.C., 2013. Model-based evaluation of maturity type of potato using a diverse set of standard cultivars and a segregating diploid population. Potato Res. 56, 127–146.

Kirk, W.W., Marshall, B., 1992. The influence of temperature on leaf development and growth in potatoes in controlled environments. Ann. Appl. Biol. 120, 511–525.

Kooman, P.L., Rabbinge, R., 1996. An analysis of the relation between dry matter allocation to the tuber and earliness of a potato crop. Ann. Bot. 77, 235–242.

Lander, E.S., Botstein, D., 1989. Mapping Mendelian factors underlying quantitative traits using RFLP linkage maps. Genetics 121, 185–199.

Lark, K.G., Chase, K., Adler, F., Mansur, L.M., Orf, J.H., 1995. Interactions between quantitative trait loci in soybean in which trait variation at one locus is conditional upon specific allele at another. Proc. Nat. Acad. Sci. U. S. A. 92, 4656–4660.

Lynch, M., Walsh, B., 1998. Genetics and Analysis of Quantitative Traits. Sinauer Associates, Sunderland, MA.

Marinus, J., Bodlaender, K.B.A., 1975. Response of some potato varieties to temperature. Potato Res. 18, 189–204.

Martin, R.J., 1995. The effect of nitrogen fertilizer on the recovery of nitrogen by a potato crop. Proc. Ann. Conf. Agron. Soc. New Zealand 25, 97–104.

Messina, C., Hammer, G., Dong, Z., Podlich, D., Cooper, M., 2009. Modelling crop improvement in a G × E × M framework via gene-trait phenotype relationships. In: Sadras, V.O., Calderini, D. (Eds.), Crop Physiology: Applications for Genetic Improvement and Agronomy. Elsevier, The Netherlands, pp. 235–265.

Meyer, K., 1985. Maximum likelihood estimation of variance components of variance components for a multivariate mixed model with equal design matrices. Biometrics 41, 153–165.

Moll, A., Klemke, T., 1990. A simple model for the evaluation of haulm characters in potato breeding. Archiv für Züchtungsforschung 20, 151–158.

Morrell, C.H., 1998. Likelihood ratio testing of variance components in the linear mixed effects model using restricted maximum likelihood. Biometrics 54, 1560–1568.

Oberhagemann, P., Chatot-Balandras, C., Bonnel, E., Schäfer-Pregl, R., Wegener, D., Palomino, C., Salamini, F., Gebhardt, C., 1999. A genetic analysis of quantitative resistance to late blight in potato: towards marker assisted selection. Mol. Breed. 5, 399–415.

Orf, J.H., Chase, K., Adler, F.R., Mansur, L.M., Lark, K.G., 1999. Genetics of soybean agronomic traits: II. Interactions between yield quantitative trait loci in soybean. Crop Sci. 39, 1652–1657.

Ospina, C.A., Lammerts van Bueren, E.T., Allefs, J.J.H.M., Engel, B., van der Putten, P.E.L., van der Linden, C.G., Struik, P.C., 2014. Diversity of crop development traits and nitrogen use efficiency among potato cultivars grown under contrasting nitrogen regimes. Euphytica 199, 13–29.

Pashiardis, S.M., 1987. Improvements of potato yield. Potato Agrometeorol. Acta Hort. 214, 27–45.

Payne, R.W., Murray, D.A., Harding, S.A., Baird, D.B., Soutar, D.M., 2009. GenStat for Windows, 12th edition. Introduction. VSN International, Hemel, Hempstead.

Perumal, N.K., Sahota, T.S., 1986. Investigations on growth and tuberization of potato at different planting dates and nitrogen levels. Int. J. Trop. Agric. 4, 63–72.

Rouppe Van der Voort, J., Wolters, J.P., Folkertsma, R., Hutten, R., Van Zandvoort, P., Vinke, H., Kanyuka, K., Bendahmane, A., Jacobsen, E., Janssen, R., Bakker, J., 1997. Mapping of the cyst nematode resistance locus Gpa2 in potato using a strategy based on comigrating AFLP markers. Theor. Appl. Genet. 95, 874–880.

Santeliz, G., Ewing, E.E., 1981. Effects of nitrogen fertilization on growth and development of potatoes. Am. Potato J. 58, 517–518.

SAS Institute Inc, 2004. SAS 9.1.3 Help and Documentation. SAS Institute Inc., Cary, NC.

Schittenhelm, S., Sourell, H., Löpmeier, F.-J., 2006. Drought resistance of potato cultivars with contrasting canopy architecture. Eur. J. Agron. 24, 193–202.

Sharma, S.K., Bolser, D., de Boer, J., Sønderkær, M., Amoros, W., Carboni, M.F., D'Ambrosio, J.M., de la Cruz, G., Di Genova, A., Douches, D.S., Eguiluz, M., Guo, X., Guzman, F., Hackett, C.A., Hamilton, J.P., Li, G., Li, Y., Lozano, R., Maass, A., Marshall, D., Martinez, D., McLean, K., Mejía, N., Milne, L., Munive, S., Nagy, I., Ponce, O., Ramirez, M., Simon, R., Thomson, S.J., Torres, Y., Waugh, R., Zhang, Z., Huang, S., Visser, R.G.F., Bachem, C.W., Sagredo, B., Feingold, S.E., Orjeda, G., Veilleux, R.E., Bonierbale, M., Jacobs, J.M., Milbourne, D., Martin, D.M., Bryan, G.J., 2013. Construction of reference chromosome-scale pseudomolecules for potato: integrating the potato genome with genetic and physical mapss. G3: Genes, Genomes, Genetics 3 (11), 2031–2047.

Sokal, R.R., Rohlf, F.J., 1995. Biometry. Freeman, San Francisco.

Spitters, C.J.T., 1988. An analysis of variation in yield among potato cultivars in terms of light absorption, light utilization and dry matter partitioning. Acta Hort. 214, 71–84.

Struik, P.C., 2007. Responses of the potato plant to temperature. In: Vreugdenhil, D., Bradshaw, J., Gebhardt, C., Govers, F., Taylor, M., MacKerron, D. (Eds.), Potato Biology and Biotechnology: Advances and Perspectives. Elsevier, pp. 367–393.

Struik, P.C., Ewing, E.E., 1995. Crop physiology of potato (*Solanum tuberosum*): responses to photoperiod and temperature relevant to crop modelling. In: Haverkort, A.J., MacKerron, D.K.L. (Eds.), Ecology and Modelling of Potato Crops Under Conditions Limiting Growth. Kluwer Academic Publishers, Dordrecht, pp. 19–40.

Struik, P.C., Geertsema, J., Custers, C.H.M.G., 1989. Effects of shoot, root and stolon

temperature on the development of the potato (*Solanum tuberosum* L.) plant: I. Development of the haulm. Potato Res. 32, 133–141.
Struik, P.C., Haverkort, A.J., Vreugdenhil, D., Bus, C.B., Dankert, R., 1990. Manipulation of tuber-size distribution of a potato crop. Potato Res. 33, 417–432.
Stuber, C.W., Polacco, M., Senior, M.L., 2003. Synergy of empirical breeding, marker-assisted selection, and genomics to increase crop yield potential. Crop Sci. 39, 1571–1583.
Sullivan, D.M., McQueen, J.P.G., Horneck, D.A., 2008. Estimating Nitrogen Mineralization in Organic Potato Production. Oregon State University Extension Service, pp. EM 8949-E.
Tardieu, F., 2003. Virtual plants: modelling as a tool for the genomics of tolerance to water deficit. Trends Plant Sci. 8, 9–14.
Tardieu, F., Tuberosa, R., 2010. Dissection and modelling of abiotic stress tolerance in plants. Curr. Opin. Plant Biol. 13, 206–212.
Tarn, T.R., Tai, G.C.C., de Jong, H., 1992. Breeding potatoes for long day, temperate climates. Plant Breeding Rev. 9, 217–332.
Tourneux, C., Devaux, A., Camacho, M.R., Mamani, P., Ledent, J.F., 2003. Effects of water shortage on six potato genotypes in the highlands of Bolivia (I): morphological parameters, growth and yield. Agronomie 23, 169–179.
Van Delden, A., Kropff, M.J., Haverkort, A.J., 2001. Modeling temperature- and radiation-driven leaf area expansion in the contrasting crops potato and wheat. Field Crops Res. 72, 119–142.
Van der Beek, J.G., Verkerk, R., Zabel, P., Lindhout, P., 1992. Mapping strategy for resistance genes in tomato based on RFLPs between cultivars: Cf-9 (resistance to *Cladosporium fulvum*) on chromosome 1. Theor. Appl. Genet. 84, 106–112.
Van der Wal, A.F., Bouma, W.F., Huijsman, C.A., Maris, B., Van Suchtelen, N.J., Wiersema, H.T., 1978. Breeding to maximize the physiological potential of potatoes for yield. Survey Papers 7th Triennial Conference EAPR 23–33.
Van der Zaag, D.E., 1982. 3. Water Supply to Potato Crops. Netherlands Potato Consultative Institute and Ministry of Agriculture and Fisheries, pp. 20–21.
Vander Zaag, P., Demagante, A.L., 1987. Potato (*Solanum* spp.) in an isohyperthermic environment. I. Agronomic management. Field Crops Res. 17, 199–217.
Van Eeuwijk, F.A., 2003. Genotype by environment interaction - basics and beyond. Plant Breeding: The Arnel R. Hallauer International Symposium.
Van Eeuwijk, F.A., Malosetti, M., Yin, X., Struik, P.C., Stam, P., 2005. Statistical models for genotype by environment data: from conventional ANOVA models to eco-physiological QTL models. Austr. J. Agric. Res. 56, 883–894.
Van Oijen, M., 1991. Light use efficiencies of potato cultivars with late blight (*Phytophthora infestans*). Potato Res. 34, 123–132.
Van Ooijen, J.W., 2006. JoinMap 4.1, Software for the Calculation of Genetic Linkage Maps in Experimental Populations. Plant Research International, Wageningen.
Van Os, H., Andrzejewski, S., Bakker, E., Barrena, I., Bryan, G.J., Caromel, B., Ghareeb, B., Isidore, E., De Jong, W., Van Koert, P., Lefebvre, V., Milbourne, D., Ritter, E., Rouppe van der Voort, J.N.A.M., Rousselle-Bourgeois, F., Van Vliet, J., Waugh, R., Visser, R.G.F., Bakker, J., Van Eck, H.J., 2006. Construction of a 10,000-marker ultradense genetic recombination map of potato: providing a framework for accelerated gene isolation and a genome wide physical map. Genetics 173, 1075–1087.
Visker, M.H.P.W., Keizer, L.C.P., Van Eck, H.J., Jacobsen, E., Colon, L.T., Struik, P.C., 2003. Can the QTL for late blight resistance on potato chromosome 5 be attributed to foliage maturity type? Theor. Appl. Genet. 106, 317–325.
Voorrips, R.E., 2002. Map Chart: software for the graphical presentation of linkage maps and QTLs. J. Hered. 93, 77–78.
Vos, J., 1995a. Foliar development of the potato plant and modulations by environmental factors. In: Kabat, P., van den Broek, B.J., Marshall, B., Vos, J. (Eds.), Modelling and Parameterization of the Soil-Plant-Atmosphere System. A Comparison of Potato Growth Models. Wageningen Pers, Wageningen, pp. 21–38.
Vos, J., 1995b. Nitrogen and the growth of potato crops. In: Haverkort, A.J., MacKerron, D.K.L. (Eds.), Potato Ecology and Modelling of Crops Under Conditions Limiting Growth. (Current Issues in Production Ecology). Kluwer Academic Publishers, Dordrecht, The Netherlands, pp. 115–128.
Vos, J., 2009. Nitrogen responses and nitrogen management in potato. Potato Res. 52, 305–317.
Vos, J., Biemond, H., 1992. Effects of nitrogen on the development and growth of the potato plant: I. Leaf appearance, expansion growth, life spans of leaves and stem branching. Ann. Bot. 70, 27–35.
Vos, J., Groenwold, J., 1989. Genetic differences in water-use efficiency, stomatal conductance and carbon isotope fractionation in potato. Potato Res. 32, 113–121.
Vos, P., Hogers, R., Bleeker, M., Reijans, M., van der Lee, T., Hornes, M., Friters, A., Pot, J., Paleman, J., Kuiper, M., Zabeau, M., 1995. AFLP: a new technique for DNA fingerprinting. Nucl. Acids Res. 23, 4407–4414.
Xu, X., Pan, S., Cheng, S., Zhang, B., Mu, D., Ni, P., Zhang, G., Yang, S., Li, R., Wang, J., Orjeda, G., Guzman, F., Torres, M., Lozano, R., Ponce, O., Martinez, D., De la Cruz, G., Chakrabarti, S.K., Patil, V.U., Skryabin, K.G., Kuznetsov, B.B., Ravin, N.V., Kolganova, T.V., Beletsky, A.V., Mardanov, A.V., Di Genova, A., Bolser, D.M., Martin, D.M., Li, G., Yang, Y., Kuang, H., Hu, Q., Xiong, X., Bishop, G.J., Sagredo, B., Mejía, N., Zagorski, W., Gromadka, R., Gawor, J., Szczesny, P., Huang, S., Zhang, Z., Liang, C., He, J., Li, Y., He, Y., Xu, J., Zhang, Y., Xie, B., Du, Y., Qu, D., Bonierbale, M., Ghislain, M., del Rosario Herrera, R., Giuliano, G., Pietrella, M., Perrotta, G., Facella, P., O'Brien, K., Feingold, S.E., Barreiro, L.E., Massa, G.A., Diambra, L., Whitty, B.R., Vaillancourt, B., Lin, H., Massa, A.N., Geoffroy, M., Lundback, S., DellaPenna, D., Buell, C.R., Sharma, S.K., Marshall, D.F., Waugh, R., Bryan, G.J., Destefanis, M., Nagy, I., Milbourne, D., Thomson, S.J., Fiers, M., Jacobs, J.M., Nielsen, K.L., Sønderkær, M., Iovene, M., Torres, G.A., Jiang, J., Veilleux, R.E., Bachem, C.W., de Boer, J., Borm, T., Kloosterman, B., van Eck, H., Datema, E., te Lintel Hekkert, B., Goverse, A., van Ham, R.C., Visser, R.G.F., 2011. Genome sequence and analysis of the tuber crop potato. Nature 475 (7355), 189–195.
Yin, X., Goudriaan, J., Lantinga, E.A., Vos, J., Spiertz, J.H.J., 2003. A flexible sigmoid function of determinate growth. Ann. Bot. 91, 361–371.
Yin, X., Guo, W., Spiertz, J.H.J., 2009. A quantitative approach to characterize sink-source relationships during grain filling in contrasting wheat genotypes. Field Crops Res. 114, 119–126.
Yin, X., Kropff, M.J., McLaren, G., Visperas, R.M., 1995. A nonlinear model for crop development as a function of temperature. Agric. Forest Meteorol. 77, 1–16.
Yin, X., Kropff, M.J., Stam, P., 1999a. The role of ecophysiological models in QTL analysis: the example of specific leaf area in barley. Heredity 82, 415–421.
Yin, X., Stam, P., Dourleijn, C.J., Kropff, M.J., 1999b. AFLP mapping of quantitative trait loci for yield-determining physiological characters in spring barley. Theor. Appl. Genet. 99, 244–253.
Yin, X., Struik, P.C., 2008. Applying modelling experiences from the past to shape crop systems biology: the need to converge crop physiology and functional genomics. NewPhytol. 179, 629–642.
Yin, X., Struik, P.C., 2010. Modelling the crop: from system dynamics to systems biology. J. Exp. Bot. 61, 2171–2183.
Yin, X., Struik, P.C., Kropff, M.J., 2004. Role of crop physiology in predicting gene-to-phenotype relationships. Trends Plant Sci. 9, 426–432.
Yin, X., Struik, P.C., Van Eeuwijk, F.A., Stam, P., Tang, J., 2005. QTL analysis and QTL-based prediction of flowering phenology in recombinant inbred lines of barley. J. Exp. Bot. 56, 967–976.
Yin, X., Van der Linden, C.G., Struik, P.C., 2018. Bringing genetics and biochemistry to crop modelling, and vice versa. Eur. J. Agron. 100, 132–140.
Zeng, Z.B., 1994. Precision mapping of quantitative trait loci. Genetics 136, 1457–1468.